In: The Visual Neurosciences; Chapter 17 pp. 234-259
L.M. Chalupa, J.S. Werner, editors
MIT Press, Cambridge MA

17 How Retinal Circuits Optimize the Transfer of Visual Information

PETER STERLING

What it means to "understand" the retina

The retina is a thin sheet of *brain* tissue (100 to 250 µm thick) that grows out into the eye to provide neural processing for photoreceptor signals (Fig. 17.1). In cats and macaque monkeys, it weighs about 0.1 g and covers 800 mm^2, about twice the area of a U.S. quarter (Packer et al., 1989). The retina includes both photoreceptors and the first two to four stages of neural processing. Its output projects centrally over many axons (1.6×10^5 in cats [Williams et al., 1993]; 1.3×10^6 in humans, and 1.8×10^6 in macaques [Potts et al., 1972]), and analysis of these information channels occupies about half of the cerebral cortex (van Essen et al., 1992; Baseler et al., 2002). Because the retina constitutes a significant fraction of the brain (roughly 0.3%), to "solve" it completely would be a significant achievement for neuroscience. This overview considers what a "solution" would entail and summarizes progress toward that goal.

First, we need the basic patterns of connection. The retina's two synaptic layers span only 60 µm, and most lateral processes span only tens to hundreds of micrometers (versus millimeters to centimeters in cortex). Therefore, it has proved technically straightforward to identify, trace, and quantify the neurons and many of their synaptic connections. This approach has revealed that the retina comprises about 75 discrete neuron types connected in specific, highly stereotyped patterns. Second, we need the "neurochemical architecture". Although information is far from complete, the main neurotransmitters and their receptor types have been identified with the key cell types and synapses. Third, we need the basic response of each cell type. Because the intact retina can be maintained in vitro, a cell's light response can be recorded and the cell filled with dye to determine its morphology. This has permitted the neuroanatomical/neurochemical connections to be interpreted as functional "circuits" (Fig. 17.2).

Such circuits explain both intrinsic retinal mechanisms and also visual performance. For example, known circuits can explain reasonably well how a ganglion cell achieves its "center-surround" receptive field, and how one type of ganglion cell produces a linear, sustained response while a different type yields a nonlinear, transient response. Still other circuits explain how, at night a ganglion cell manages to fire 2 to 3 spikes to a single photon, while by day it fires a similar number of spikes to an increment of 10^5 photons. Finally, we know how different retinal circuits specialize for spatial acuity, motion, and opponent perception of hue (Calkins and Sterling, 1999; Wässle and Boycott, 1991).

CROSSING FROM "HOW" TO "WHY" Deep understanding of any brain region requires that one go beyond mechanism (*how*) to consider the computational purpose (*why*). For instance, why do we need a neural processor within the eye—since all other sense organs transmit spikes directly to the brain (Fig. 17.3)?

And what explains the particularities of retinal design? For example, why are mammalian photoreceptors small, whereas in many cold-blooded species, they are large? And why do photoreceptor and bipolar cells use presynaptic "ribbons," since these are absent from the brain itself?

Many biologists dislike asking "why?" because it can be hard to prove that a given feature is truly adaptive, rather than merely decorative or a historical leftover of some evolutionary/developmental program (Gould and Lewontin, 1979). For engineers, however, "why" is no problem. Every aspect of their design implies some specification of performance, constraints in cost (energy, materials, labor), and many compromises. If engineers understand their design, they can explain *exactly why* their bridge was built a particular way (Petroski, 1996; Glegg, 1969). If they cannot explain this, stay off that bridge! So, the ability to answer "why" measures the depth of our comprehension.

Another test of comprehension is to ask whether circuit components *match optimally*, a condition termed "symmorphosis" (Diamond, 1992, 1993; Diamond and Hammond, 1992; Taylor and Weibel, 1981; Weibel, 2000). Where a neural system can be shown to satisfy the principle of symmorphosis across many levels (behavior ↔ circuit ↔ cells ↔ molecules), it can be chalked up as virtually understood. Many biologists do not care for this question either, reasoning that because evolution is ceaseless, how can one know whether a given feature has reached optimality?

But when a mechanism is shown to meet some physical limit, such as diffraction or diffusion, then natural selection

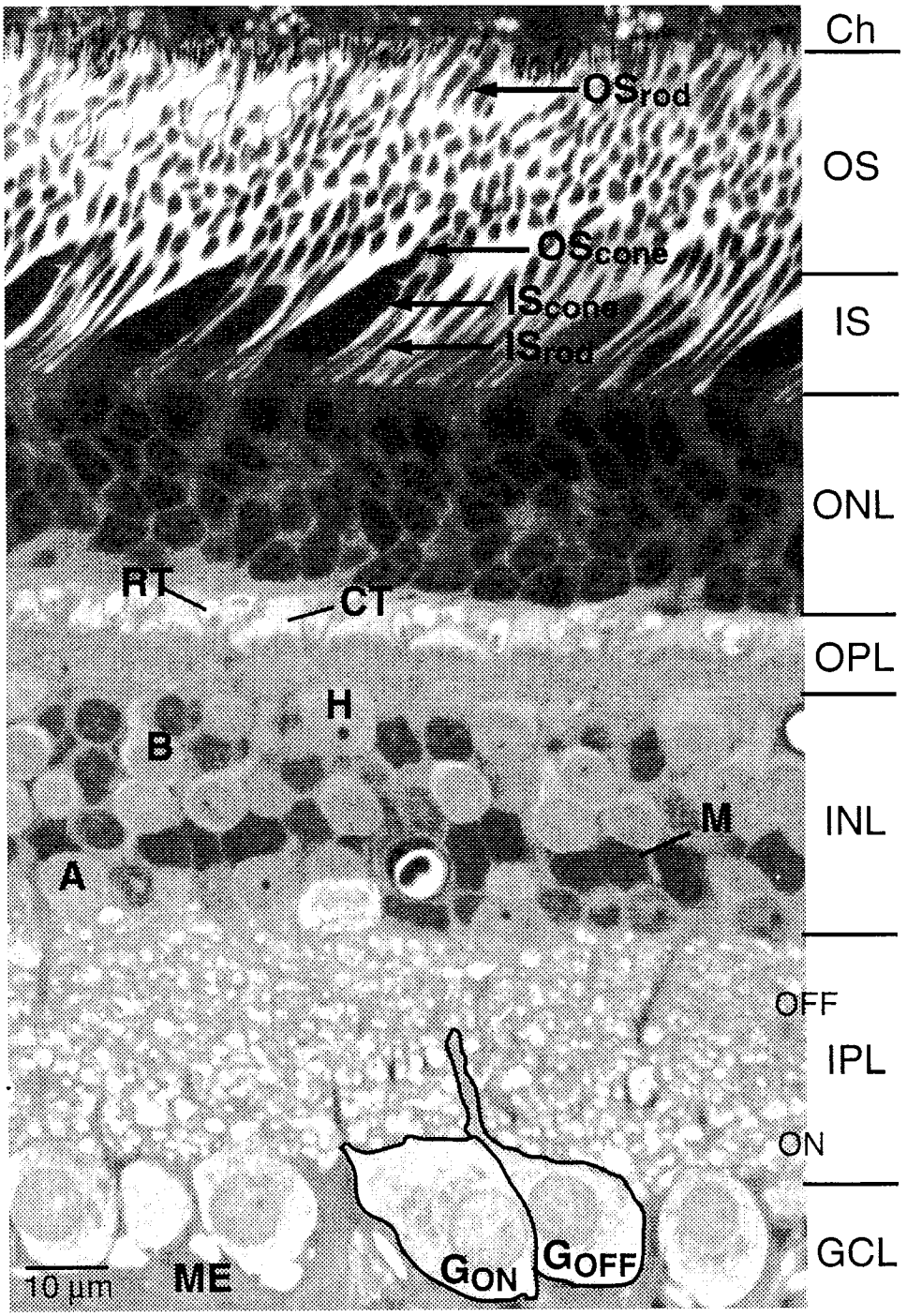

FIGURE 17.1. Radial section through monkey retina about 5 mm (~25 degrees) from the fovea. The synaptic layers span only 60 µm. Cone and rod inner segments are easily distinguished from each other, as are their terminals in the outer plexiform layer. Pigmented cells of the choroid layer (Ch) convert vitamin A to its photoactive form and return it to the outer segments. Pigmented cells also phagocytose membrane discs that are shed daily from the outer segment tips. OS, outer segment; IS, inner segment; ONL, outer nuclear layer; CT, cone terminal; RT, rod terminal; OPL, outer plexiform layer; INL, inner nuclear layer; IPL, inner plexiform layer; GCL, ganglion cell layer; B, bipolar cell; M, Müller cell; H, horizontal cell; A, amacrine cell; ME, Müller end feet; G_{ON} and G_{OFF}, ganglion cells. (Light micrograph by N. Vardi; modified from Sterling, 1998.)

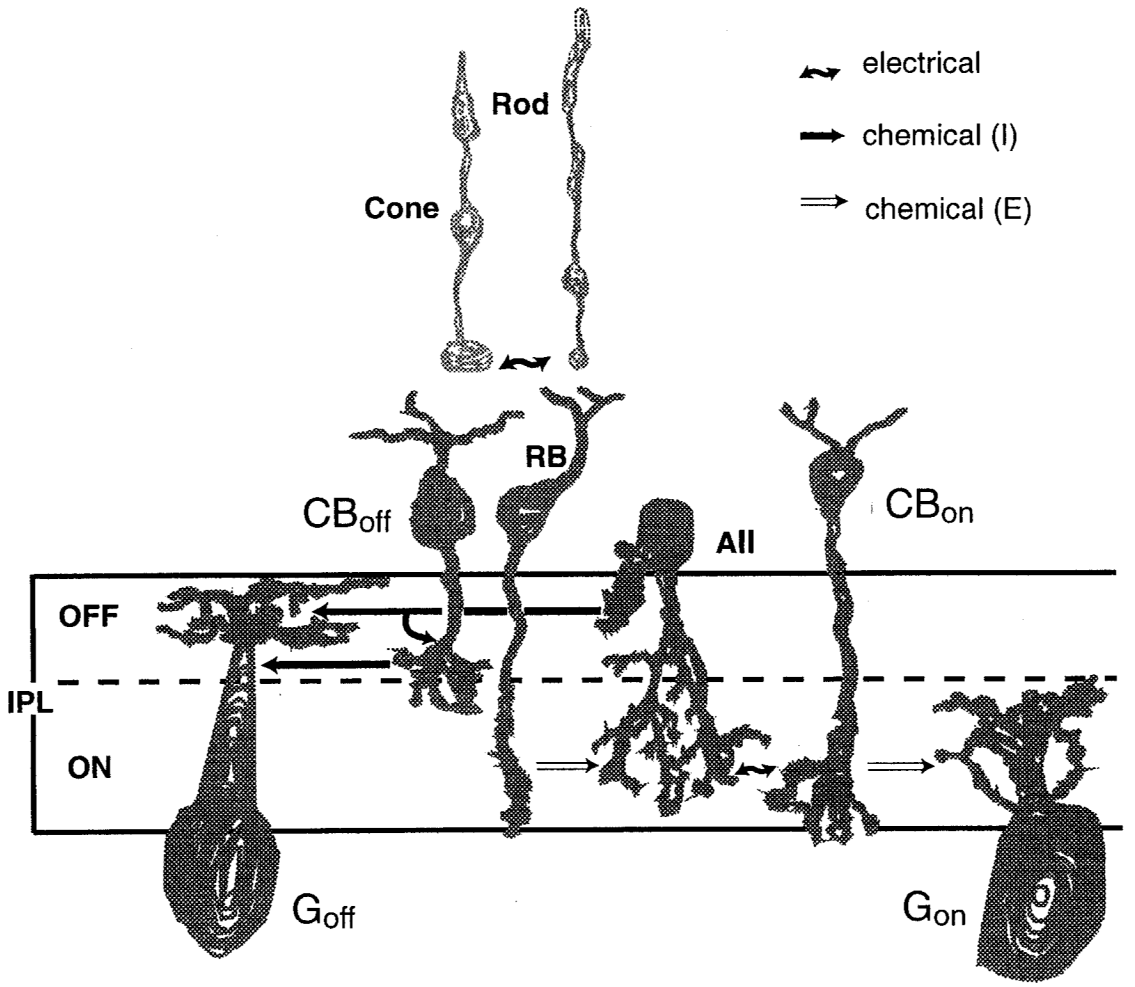

FIGURE 17.2. The basic circuits that relay rod and cone signals through the retina to ganglion cells are known. Cone signals modulate ON and OFF cone bipolar cells (CB) that excite ON and OFF ganglion cells (GC). Rod signals modulate cone terminals via electrical synapse and relay single photon signals via a private rod bipolar cell (RB) that excites the AII amacrine cell. The AII is bifunctional, inhibiting the OFF ganglion cell with glycine and exciting the ON ganglion cell via electrical synapse to the ON bipolar terminal. IPL, inner plexiform layer. (Modified from Sterling, 1998.)

has clearly hit the wall. And where several physical constraints conflict, neural design must reflect their compromise. In short, where actual performance approaches "ideal" performance calculated from physical limits, there is a genuine opportunity to address the "why" of a design. Although for most brain regions this is a distant goal, for mammalian retina such questions can now be addressed, and they provide the framework for this overview.

Consider that in nature the visual system operates near threshold. This is easily forgotten living under artificially bright light and viewing mostly high contrast images, such as newsprint or the computer screen. But go bird watching or hunting (heaven forbid!), and you are quickly reminded that our ancestors strained to see the finest detail at the lowest contrast in the poorest light. To maximize sensitivity their eyes were selected to make each stage—from the optical image to the ganglion cell spike train—as efficient as possible. Thus each stage should approach the limits set by physical laws and by compromises required by the organism's "niche." Thus *every stage* is a potential "bottleneck," and the purpose at each stage must be to staunch the loss of information up to the physical limit. This hypothesis sets a framework for interpreting the functional architecture.

The central idea of this chapter is that the retina evolved to maximally extract information from the natural spatiotemporal distribution of photons and to convey this information centrally, with minimal loss. Upon this broad goal there are functional constraints: cover a wide range of intensities (10^{10}); respond to very low contrasts (~1%); integrate for short times (~0.1 second); keep tissue thin (~0.2 mm), and maintain the metabolic rate no higher. There are also basic constraints on biological computation: signal amplitude and velocities are set by properties of biological membranes and

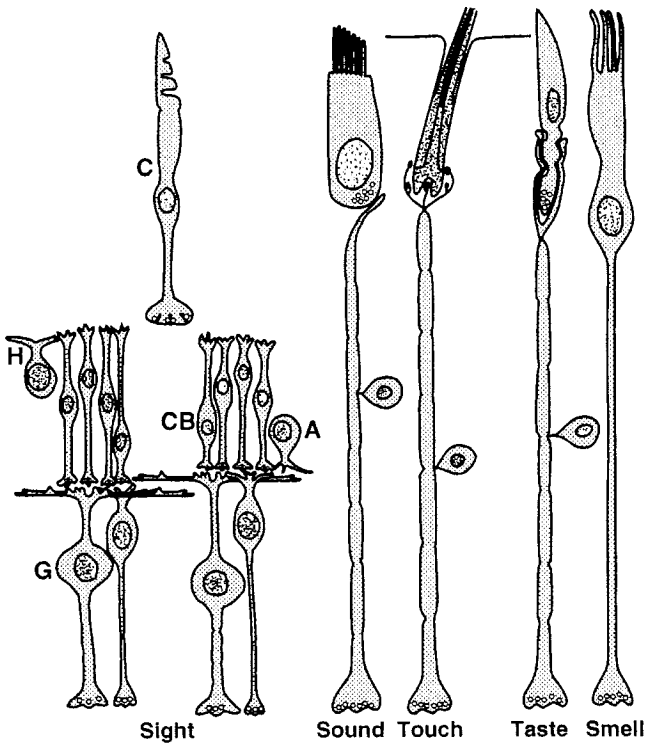

FIGURE 17.3. Only the visual sense requires neural processing at the site of transduction. The mammalian cone (*upper left*) requires lateral integration at its output (horizontal cells [H]), followed by 8 to 10 parallel circuits for a second stage (cone bipolar cells [CB]). Then, it requires more lateral integration (amacrine cells [A]) and finally, 10 to 20 parallel lines (four are shown; ganglion cells [G]) to carry action potentials to the brain. This chapter considers why photoreceptors require such extensive integration and so many parallel circuits before projecting centrally.

the speed of aqueous diffusion; accuracy and reliability of synaptic transmission are constrained by its quantal and Poisson nature. The retina's functional architecture reflects numerous compromises shaped by the interplay of these major factors as they contribute to the organism's overall success in its environment.

WHY NATURAL IMAGES NEED LOTS OF LIGHT Both prey and predators try to merge with the background, so in nature contrast for significant objects tends to be low. Consider the bighorn sheep among the cottonwoods (Fig. 17.4*A*). The retinal image is represented as peaks and troughs of intensity that differ from the local mean by only ~20%, and much fine structure exhibits far lower contrast, only a few percent (Fig. 17.4*B*). This range is common in nature (Laughlin, 1994; Srinivasan et al., 1982), and thus our visual threshold for a small stimulus, such as one spanning a single ganglion cell dendritic field, is ~3% contrast (Watson et al., 1983; Dhingra et al., 2003).

To create an optical image at low contrast requires many photons (Rose, 1973; Snyder et al., 1977). Because light is quantized, a small difference from the mean, say 1%, implies that the mean itself must contain at least 100 photons. But photons at each image point arrive randomly in time (Poisson distribution). So even when an image is perfectly still on the retina, the intensity at every point *varies* temporally, with a standard deviation equal to the square root of the mean. Because the minimum detectable contrast (Δn) must differ from the mean by at least one standard deviation, the ability to detect a contrast of 1% implies a mean of at least 10,000 photons:

$$\Delta n/n > \sqrt{n}/n = 100/10{,}000 = 1\%$$

This root-mean-square fluctuation ($\sqrt{n}$) is termed "photon noise."

One might think that daylight would provide plenty of photons to represent any scene. However, this depends on the extent of photon integration; fine spatial detail implies limited spatial pooling and thus relatively large fluctuations from photon noise (Fig. 17.5*A*). This might be avoided by increasing temporal integration, but because mammals move swiftly, prolonged integration would blur the spatial image. Thus temporal integration is constrained to ~100 msec (Schneeweis and Schnapf, 1995). Although daylight contains enough photons/100 msec to cast a fine image on the cornea, the excess is not large, nor does it extend to even slightly dimmer situations, for example, when a cloud obscures the sun. The need for intense light to register fine detail at low contrast partly explains why athletes, bird watchers, etc. do not wear sunglasses (Sterling et al., 1992).

Mammalian photoreceptor mosaic

THE NEED FOR TWO TYPES OF DETECTOR The photoreceptor mosaic is optimized to cover the full range of environmental light intensities (10^{10}). This design specification requires two types of detector with different sensitivities, the rod and the cone (see Figs. 17.1, 17.5, and 17.6).[1] The rod serves under starlight where photons are so sparse that over 0.2 second (the rod integration time), they cause only ~1 photoisomerization (R*)/10,000 rods. Consequently, under starlight and for 3 log units brighter, a rod must give a *binary* response, reporting over each integration time the

[1] Of course, insects cover the same intensity range with a single type of photoreceptor, but they differ in many respects, including basic optical design, regeneration of rhodopsin, and use of an entirely differentransduction cascade. When insect phototransduction is finally worked out, we may understand better how it manages to compress the full intensity range into a single cell type.

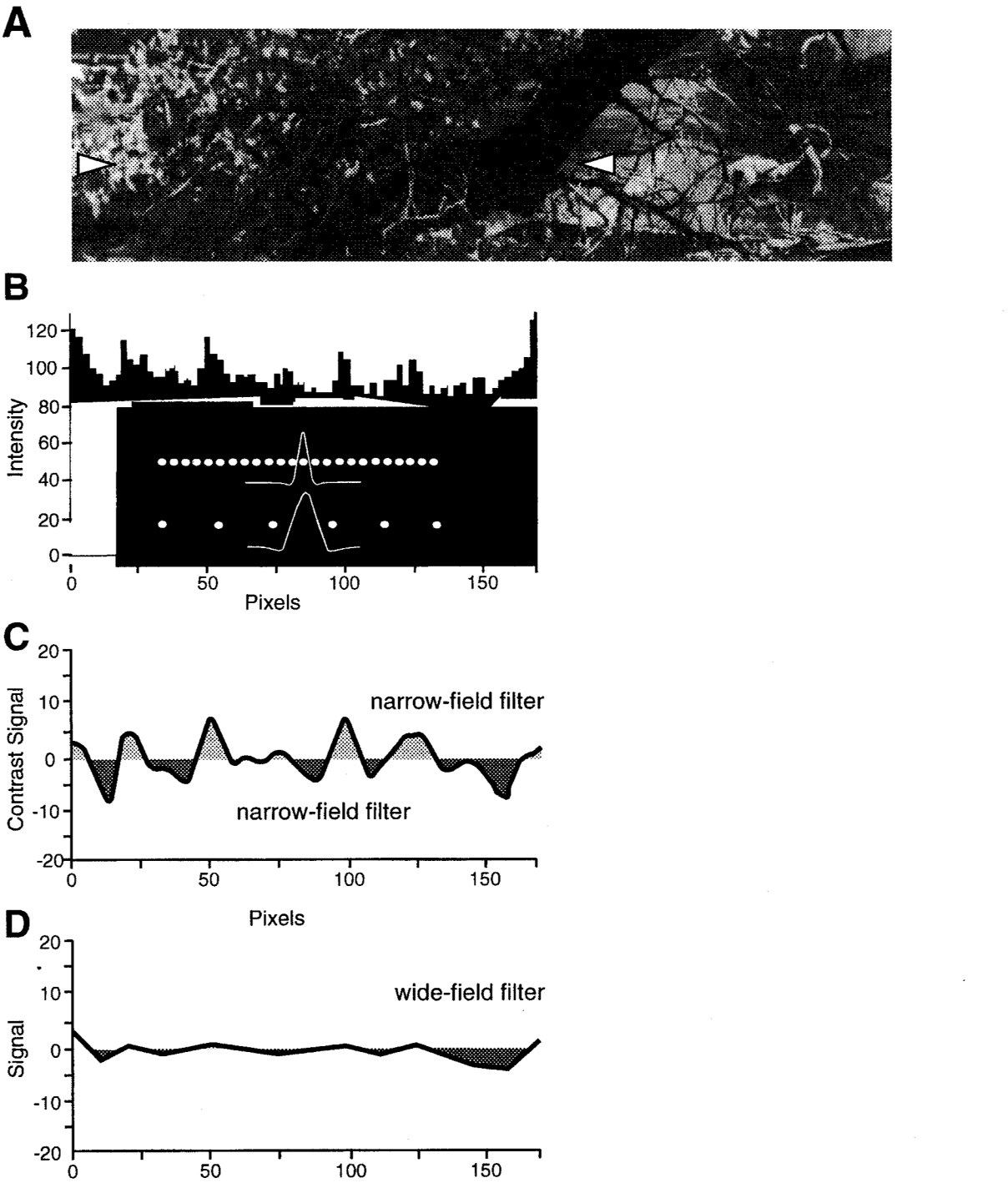

FIGURE 17.4. How narrow-field and wide-field ganglion cell arrays "filter" the transduced image of a natural scene. *A*, Photograph of a bighorn sheep among the cottonwoods. Spatial detail is represented as peaks and troughs of intensity around some mean level (arrowheads mark the area scanned in *B*). *B*, Photometer scan across the middle of the image. Much discernible structure, e.g., fine branches, differs from the mean by only a few percent. Were this scene viewed by a cat at 10 meters, 1 pixel would correspond roughly to one cone, and the intensity axis would correspond roughly to the signal amplitude across the cone array. Dimensions and spacings of the narrow and wide receptive fields are also indicated. *C*, Signal amplitude after filtering by narrow-field array. Subtraction by the surrounds of the shared signal component has reset the mean to zero: pooling by the centers has removed the noisy fluctuations. *D*, Signal amplitude after filtering by the wide-field cell array. Again, a zero mean, but the broad pooling and sparse sampling has removed all but the coarsest spatial detail—thereby clearing the wide-field cell dynamic range to efficiently encode motion. (Photograph by A. Pearlman; computations for *B to D* by R. Rao-Mirotznik and M. Eckert; modified from Sterling, 1998.)

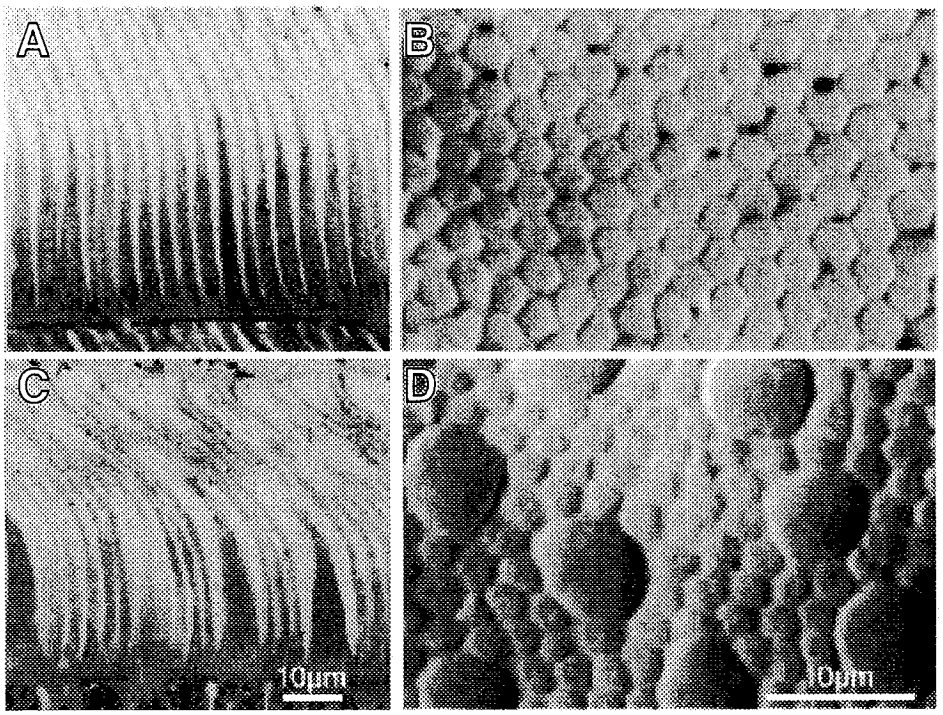
A
B
C
D
10μm
10μm

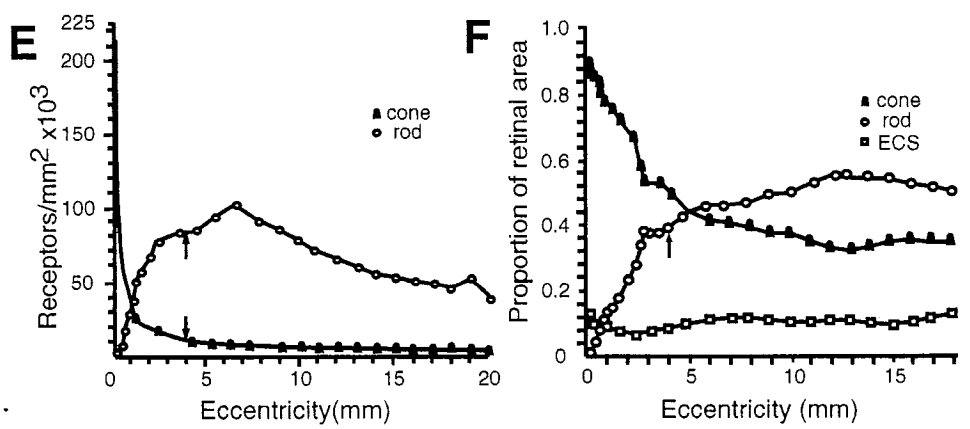
E
Receptors/mm2 x10-3
225
200
150
100
50
cone
rod
0
5
10
15
20
Eccentricity(mm)
F
Proportion of retinal area
1.0
0.8
0.6
0.4
0.2
0
cone
rod
ECS
0
5
10
15
Eccentricity (mm)

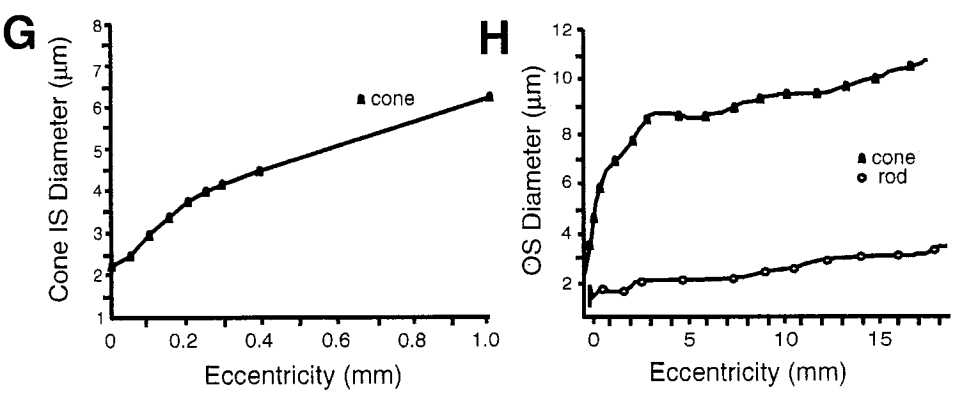
G
Cone IS Diameter (μm)
8
7
6
5
4
3
2
1
cone
0
0.2
0.4
0.6
0.8
1.0
Eccentricity (mm)
H
OS Diameter (μm)
12
10
8
6
4
2
cone
rod
0
5
10
15
Eccentricity (mm)

occurrence of either 0 or 1 R*. The rod continues to serve at dawn (or twilight) as photons arrive more densely, providing more than one R*/integration time. The rod sums these linearly up to 20 R*/integration time and then gradually saturates, with 100 R* evoking a maximal photocurrent of ~20 pA. Under steady light, the rod adapts (reduces gain), and this allows it to continue signaling up to ~1000 R*/rod/integration time (Nakatani et al., 1991).

The cone serves under full daylight, beginning when photon density reaches ~100 photons/receptor/integration time. The cone actually absorbs and transduces single photons, but because its gain is 50-fold lower than the rod's, it requires 100 R* for the signal to rise above the continuous dark noise. By 1000 R*/integration time, when rods are nearly saturated, the cone responds strongly. The cone photocurrent saturates at ~30 pA (similar to the rod), but this occurs at much higher intensity (Burns and Lamb, 2003). Whether the mammalian cone in situ adapts by reducing gain or simply by saturating remains uncertain, but in any case, this detector serves intensities up to 10^6 R*/cone/integration time (Pugh and Lamb, 1993; Schnapf et al., 1990). Consequently, whereas the rod signal is at first binary and then graded, but always corrupted by photon noise, the cone signal is always graded and far less noisy.

Subdividing the Receptor Mosaic How should space in the receptor mosaic be apportioned? To maximize photon capture, receptors should completely fill the plane, and they *do*, occupying 90% and leaving an irreducible 10% to narrow intercellular channels required for exchange of ions and metabolites (see Fig. 17.5). To maximize night vision, rods should fill the plane, but that would reduce daylight vision. Obviously, there can be no single "optimal" solution, but only compromises that promote survival in a given niche. For example, the ground squirrel forages only in daylight and expresses only cones. However, most mammals cover the full intensity range and express both types of receptor. Their rods always far outnumber cones, and across species (from mouse to human), the ratio is surprisingly constant, about 20 rods per cone.

That this ratio genuinely represents a compromise can be appreciated from the many interesting exceptions that have been observed (Hughes, 1977). For one example, cones in the primate fovea completely fill the plane and exclude all rods (see Fig. 17.5). This enhances spatial resolution in daylight, but once light intensity falls below 100 photons/cone/integration time, the cost is utter blindness in this retinal region. To convince yourself, wait for color to disappear at dusk, indicating loss of cone function, then extend your arm and fix steadily upon your thumb: it will disappear. This specialization for high spatial acuity requires various auxiliary modifications to the retina, mentioned in a later section.

What sets the basic ratio at 20 rods: 1 cone? For the rod system, photons are so sparse that a ganglion cell may sum signals from more than 10,000 rods, yet still be dominated by photon noise. Therefore, the rod system madly competes for territory to catch every photon. But if rods managed to capture the last 5% of the mosaic, their signal-to-noise (S:N) ratio would improve only by $\sqrt{100/95}$, or 2.6%. Of course, there would be no daylight vision. So that is the trade: sacrifice 2.6% in sensitivity at night for the advantage of excellent photodetection by day.

For the cone system, photons are relatively plentiful, so the same ganglion summing signals from only 500 cones (each transducing, say, 1000 photons) will be responding to 500,000 photons. The S:N ratio calculated for photons ($500{,}000/\sqrt{500{,}000}$) is ~700. Thus the cone-driven ganglion cell will hardly be affected by photon noise; instead its threshold is set by synaptic gain and neural noise (Dhingra et al., 2003; Freed, 2000a). Consequently for regions of the receptor mosaic where ganglion cells sum broadly, cones cannot improve vision by expanding territory, and thus they are well "satisfied" with 5%.

Where a particular species or retinal region requires higher spatial acuity, the cone territory *does* expand. Here, too, the physical constraints are known: (1) spatial acuity is set by ganglion cell sampling density because Nyquist's limit requires at least two samples for each spatial cycle (reviewed by Wässle and Boycott, 1991; Williams, 2003); (2) ganglion cell dendritic fields shrink and collect from fewer cones. Eventually photon noise reduces the ganglion cell S:N ratio, and to preserve it cones must capture more territory. For example, in peripheral cat retina, where the

Figure 17.5. The foveal receptor mosaic is optimized for spatial resolution and contrast sensitivity; the peripheral mosaic is optimized for temporal resolution by day and absolute sensitivity by night. *A*, Human fovea, radial view. Cone inner segments are narrow and gently tapered; outer segments are long and fine. *B*, Human fovea, tangential view through the base of the inner segments. Hexagonal cone packing provides the finest possible spatial sampling in daylight, but the absence of rods renders the fovea blind from dusk to dawn. *C*, Human, near periphery, radial view. Cone inner segments taper sharply and are surrounded by rod inner segments, which are much finer and untapered. *D*, Human, 20 degrees nasal, tangential view. Large cone inner segments enhance sensitivity to high temporal frequencies, yet "spill" photons at night to surrounding rods. *E to H*, See text for explanation. IS, inner segment; OS, outer segment; ECS, extracellular space. (A–D, Video-DIC images from Curcio et al., 1990; E and F, Replotted from Packer et al., 1989. Used with permission)

dendritic field of a brisk-sustained ganglion cell sums 1000 cones, the rod/cone ratio is 100. However, in the central retina, where the brisk-sustained cell dendritic field shrinks to encompass only 30 cones, the rod/cone ratio is ~10. (Cohen and Sterling, 1992; Steinberg et al., 1973; Williams et al., 1993).

WHY THE OUTER SEGMENTS OF MAMMALIAN PHOTORECEPTORS ARE UNIFORM AND SMALL Dimensions of the rod outer segment are surprisingly uniform across mammals. Length is about 20 μm: 18 to 20 μm for cow and rabbit; and 25 μm for cat, Galago (nocturnal prosimian), macaque, and human (Nakatani et al., 1991; Tamura et al., 1991). Diameter is about 1.5 μm: 1 to 1.2 μm for cat (Steinberg et al., 1973; Williams et al., 1993), Galago, and owl monkey (all nocturnal); and 1.8 to 2 μm for rabbit, macaque, and human (Curcio et al., 1987, 1990; Packer et al., 1989). Diameter is somewhat smaller in central retina: cat, 1 μm central versus 1.6 μm peripheral; diurnal primate, 2 μm central versus 4 μm peripheral (Curcio et al., 1987; Packer et al., 1989). It is curious that rods should be smaller in nocturnal species. Possibly, adaptations that enhance photon gathering in the nocturnal eye (such as a large pupil, reflective tapetum) tend to move the rod circuit away from its high gain, nonlinear regime (Field and Rieke, 2002; van Rossum and Smith, 1998). This switchover can be postponed to a higher environmental light intensity by reducing the rod collecting area.

The cone outer segment is also relatively small and invariant in volume. The shape can vary; for example, it narrows in primate fovea to enhance spatial sampling, and also lengthens (see Fig. 17.6). But calculations based on Greeff's drawings suggest that across the human retina, cone outer segment volume is constant to within a factor of 2 (see Fig. 17.6). In agreement, the outer segment volumes of isolated macaque cones, judged by their different inner segment diameters to represent all eccentricities, are small and constant: 30 ± 10 μm (Schnapf et al., 1990).

In nonmammals the outer segments can be *much* larger (Fig. 17.7*A*). Thus, length can increase by orders of magnitude, reaching 60 μm in toad and 525 μm (!) in deepsea fish (Pugh and Lamb, 1993; Rodieck, 1973). Outer segments can also be much thicker. For example, the salamander outer segment, although only 25 μm long, is 11 μm in diameter. Thus, mammalian outer segments are reduced in volume by 30- to 80-fold.

This evolutionary "miniaturization" of the mammalian outer segment certainly reduces its efficiency of photon capture. For example, a photon penetrating a primate rod is 2.4-fold less likely to be captured than a photon in a toad rod. The reason is that the membrane discs bearing rhodopsin always stack as densely as possible, 36 discs/μm (see Fig. 17.7*B*). Moreover, the number of rhodopsin molecules per μm^2 of disc membrane is always 25,000 (Liebman et al., 1987). Therefore, as a photon traverses the outer segment, its probability of striking a rhodopsin depends on the number of discs. In this respect the mammalian outer segment is clearly suboptimal, which suggests a competing design constraint.

Recall that to match the mammalian motor system, photoreceptors must be *fast*. Whereas photocurrent in the large amphibian rod rises slowly, peaking at 1 to 2 seconds and with an overall integration time of 2 to 3 seconds, with an overall integration time of 2 seconds photocurrent in the small mammalian rod rises10-fold faster, peaking at 200 msec, with an overall integration time of ~300 msec (Baylor et al., 1979; Baylor et al., 1984; Kraft et al., 1993; Nakatani et al., 1991; Tamura et al., 1991). These times are essentially identical across mammals (Nakatani et al., 1991; Tamura et al., 1991), a striking contrast to insects whose different niches require large differences in speed and numerous adaptations to achieve them (Laughlin, 1994). Photocurrent in the mammalian cone rises equally rapidly, about 2 to 3 times faster (60 to 100 msec), but the integration time is shorter (50 msec) because the recovery of the photocurrent is faster and biphasic (Schnapf et al., 1990).

Why does speed require a small outer segment? The photocurrent generated by closing a cGMP-gated cation channel depends on reducing the intracellular concentration of cGMP (Burns and Lamb, 2003). Phosphodiesterase (PDE), the enzyme that hydrolyzes cGMP, is among the fastest enzymes; its catalytic rate approaches the physical limit set by how fast cGMP can reach it by aqueous diffusion (Liebman et al., 1987; Leskov et al., 2000). Thus, evolution cannot produce a faster enzyme. However, each hydrolyzed molecule in the reduced intracellular volume more effectively reduces the *concentration* of cGMP, and this raises transduction speed by 25-fold. Another factor of 4 is explained by increased body temperature: 2-fold from faster diffusion of the transduction proteins on the disc, which causes R* to increase its encounter rate with transducin (Gt), and activated transducin (Gt*) to increase its encounter rate with PDE; another 2-fold comes from PDE's accelerated catalytic rate, due to faster diffusion.

TRANSDUCTION PROTEINS AND ION CHANNELS ARE OPTIMIZED FOR SENSITIVITY, SPEED, GAIN, AND NOISE Only 20% of the disc membrane is occupied by rhodopsin, implying that denser packing could improve photon capture (sensitivity) by 5-fold. In fact, insect rhabdomeres and bacteria do achieve crystalline packing of rhodopsin, so why hasn't evolution achieved this for vertebrate photoreceptors? Furthermore, why hasn't evolution accelerated transduction by increasing PDE density? The answers are not that "evolution is still in progress," but rather that additional factors must be optimized. For example, although rhodopsin density is too low

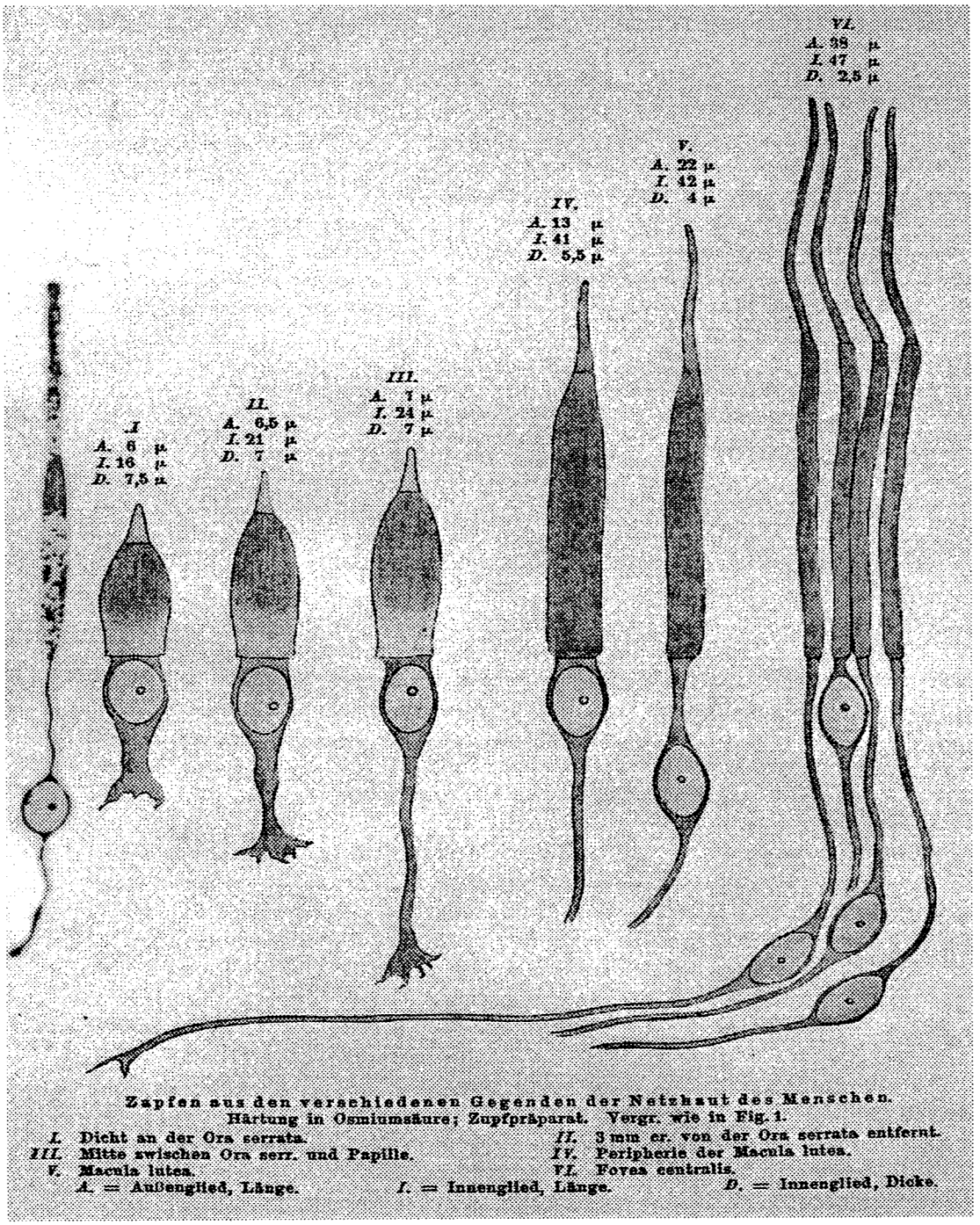

FIGURE 17.6. Cone structure varies across the retina, but rod structure is constant. Human photoreceptors dissociated and fixed with osmium. *Right-to-left:* Cones from the fovea to the periphery, plus one rod. The outer segment for the rod and foveal cone is long and columnar to maximize photon absorption; for the peripheral cone, it is short and tapered, possibly to radiate unabsorbed photons to surrounding rods (Miller and Snyder, 1973). The inner segment for the rod and foveal cone is long and columnar to allow dense packing. Photons that penetrate the cone obliquely escape, but then are captured by the densely packed, neighboring rods (see Fig. 17.5). The peripheral cone inner segment is greatly enlarged, apparently to enhance photon catch and, thus, sensitivity to motion. The axon is thick for a cone and thin for a rod (see Fig. 17.8). The cone synaptic terminal is enlarged toward the periphery; the rod terminal is small. Basal processes on the cone terminal reach out to electrically contact other cones and also rods. All of these features appear to reflect the vastly different quantities of information collected by the cone and rod and more modest differences between cones at different eccentricities. (Reprinted from Greeff, 1899.)

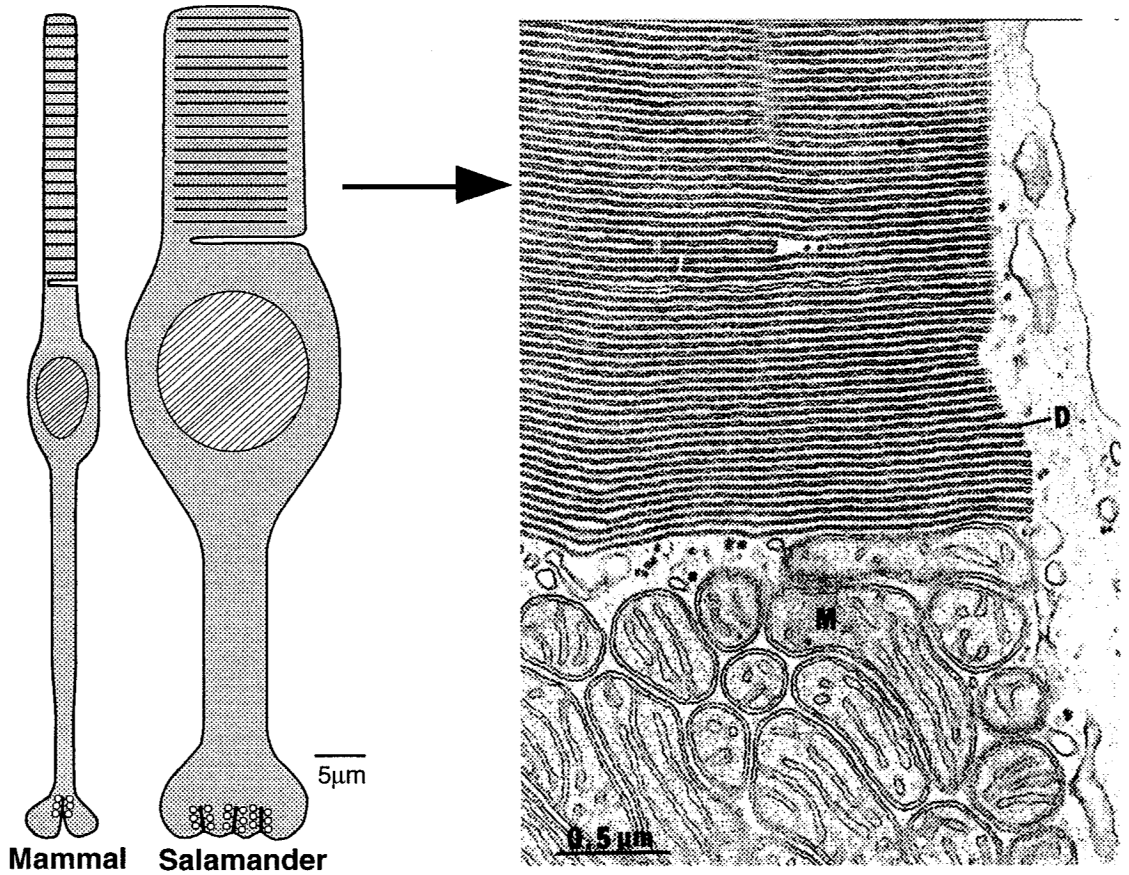

FIGURE 17.7. Mammalian rod outer segments are small in order to be fast. The mammalian outer segment must insure a high probability of encounter between a photon and a rhodopsin molecule. This is achieved by densely packing rhodopsin on both faces of a membrane disc and then stacking 900 discs at maximal density (36/μm), for a total length of ~25 μm. Although slightly longer than a salamander outer segment, the mammal's is much thinner (~1 μm vs. 11 μm in diameter). This greatly reduces its cytoplasmic volume (4% of the salamander rod). This in turn accelerates its light-evoked fall of [cGMP] by 25-fold. The mammal's higher temperature further accelerates this process by doubling the rate at which R* activates transducin (Gt) and the rate at which Gt activates phosphodiesterase (PDE). Consequently, the mammalian rod's amplification constant is about 100-fold faster, and its integration time (~200 msec) is about 10-fold shorter than the salamander rod's. The salamander rod's broader cross section and longer integration time provide it with 250-fold more R*/integration time than the mammalian rod. Consequently, its later stages are more cone-like: thicker axon, larger synaptic terminal with multiple ribbons (~8; Townes-Anderson et al., 1985), electrical coupling (Attwell, 1986); and convergence with cones onto the same bipolar cell. D, disc of outer segment; M, mitochondria of inner segment. (Electron micrograph reprinted from Townes-Anderson et al., 1995.)

for best photon catch, it is already *too high* for greatest speed because crowding slows activated rhodopsin's diffusive search for transducin. Halving rhodopsin's concentration (to 10%) in a transgenic mouse accelerates transduction speed by 1.7-fold (Calvert et al., 2001). Thus, rhodopsin's space on the disc represents an evolutionary compromise that doubles photon catch but nearly halves transduction speed.[2]

One photoisomerization (R*) in a rod triggers hydrolysis of 10^4 molecules of cGMP, leading to a photocurrent equivalent to ~10^6 monovalent ions, a gain of 1 million-fold (Burns and Baylor, 2001; Liebman et al., 1987). Gain could be increased if each step in the transduction cascade were activated for longer. But the cost would be slowing of the visual response. As it stands, one R* in a primate rod evokes a current whose average size is ~0.7 pA (Baylor et al., 1984). The event exceeds the continuous dark noise by about 5-fold, so noise as large as the photon event will occur rarely (~1% false alarms). But the S:N ratio in the mouse rod is slightly less, ~3-fold, so many photon events that are smaller than average are indistinguishable from the continuous noise

[2] Given the early evolutionary "decision" to base transduction upon multiple stages of protein-protein encounter, the hit rate is increased by restricting the diffusive search to two dimensions (on the disc), rather than three dimensions (Adam and Delbrück, 1968).

(see Fig. 17.11; Field and Rieke, 2002; Sterling, 2002). Thus, transduction, while maximizing gain, must also minimize noise due to dark fluctuations of [cGMP].

These additional specifications, plus the need for speed, define the optimal molecular ratios of the cascade's effector proteins. Each square micrometer of disk membrane bears 25,000 R:2,500 G_t:330 PDE (Lamb and Pugh, 1992). At these densities, the mean time for an R* to find a G_t by diffusive search just equals the time for which R* binds to Gt. If G_t were sparser, R*'s search would be longer. Then, depending on R*'s lifetime, either transduction would slow, or the gain would fall. On the other hand, if G_t were denser, thermal activation would rise (yielding more false alarms). Similarly, PDE is just dense enough to be efficiently activated by G_t* and sparse enough to minimize basal hydrolysis of cGMP (continuous dark noise).

The rod outer segment bears about 10^6 cGMP-gated channels, of which 10^4 are held open by the standing concentration of a few micromolar cGMP. One R* hydrolyzes about 5% of the total cGMP and thus closes about 5% of the open channels. Why should a rod express 50,000 times more channels than needed to span its dynamic range? That is, why does it express 1 million channels instead of 20? Furthermore, why express 1 million channels since, at maximal dark current, only 100,000 channels open (Yau, 1994)?

Because channels behave stochastically (like photons), the ratio of photocurrent to continuous noise (S:N) is determined by $n/\sqrt{n}$, where n = mean number of channels. Thus, 20 channels could provide an S:N ratio of ~4.5, whereas 10,000 channels could provide an S:N ratio of ~100. By requiring at most 10% of the available channels to be modulated by a given change in [cGMP], the channel's affinity for cGMP can be low, which allows a fast OFF rate, and thus rapid closure when [cGMP] falls. The channel's requirement for three cGMP molecules to open (Hill coefficient = 3) insures a steep response to small changes in [cGMP], that is, high gain (Koshland et al., 1982). Because the intrinsic channel conductance is about 20 pS, 5000 channels open in darkness might saturate the driving force. But this problem is avoided by designing the channel to be partially blocked at depolarized voltages by a magnesium ion, causing it to flicker rapidly and provide a mean functional current of 0.1 pS (Sesti et al., 1994; Yau, 1994).

The cone outer segment resembles the rod outer segment in many respects: opsin photoefficiency; speed of turn on (amplification constant); peak photocurrent; dark concentration of cGMP; number of CNG channels (Pugh and Lamb, 1993; Schnapf et al., 1990; Yau, 1994). In the cone, just like the rod, a single photon effectively triggers the transduction cascade. But, whereas one R* in a rod closes 5% of the open channels, in a cone it closes only 0.1 to 0.01% (Kraft et al., 1993; Schnapf et al., 1990). This sets the cone's gain ~50-fold lower than the rod's, rendering the cone most effective when there are more than 10^3 photons/integration time, a regime where photon S:N is high. Cone sensitivity is lower because it depends multiplicatively on the time constant of each transduction step, and all are abbreviated compared to the rod. The advantage is greater temporal resolution and thus greater bandwidth. Because information capacity in any channel rises with the log of S:N ratio and *linearly* with bandwidth (Shannon and Weaver, 1949), the cone's information capacity greatly exceeds the rod's.

WHY THE CONE INNER SEGMENT VARIES The inner segment shifts markedly across the human retina (see Figs. 17.5 and 17.6). At the fovea's center, it is tall and columnar, but across the fovea, the inner segment gradually thickens. At greater eccentricities, the inner segment becomes still broader, shorter, and tapered (quasi-ellipsoid), its aperture ultimately increasing in area by 20-fold. This shift produces concentric rings of cones with progressively greater inner segment diameter. Since the outer segments (both rod and cone) are rather constant, as is the rod inner segment, why should the cone inner segment vary?

The inner segment is crammed with mitochondria that generate ATP for the sodium/potassium transporters that maintain the circulating dark current (Fig. 17.7). But the mitochondria also enhance refractive index, and this converts the inner segment to an optical wave guide. Photons entering roughly parallel to the long axis are trapped and efficiently funneled to the outer segment (Enoch, 1981). The cone inner segments pack triangularly in fovea, so the inner segment diameter sets the number of cones per degree of visual angle and, since private lines are maintained from cone to striate cortex, this determines spatial resolution (Smallman et al., 1996). Of course, narrowing the inner segment to enhance resolution reduces photon catch and thus limits the cone's signal/noise ratio. Calculations prove that for each light level there exists an optimal balance of spatial resolution versus S:N ratio that maximizes total information (Snyder et al., 1977). Consequently the fovea's array of concentric rings with progressively larger inner segments should maximize information uptake over a range of daylight intensities.

The inner segment's marked expansion beyond the fovea further enhances photon capture (see Figs. 17.5 and 17.6). There is no cost to spatial resolution, which is set outside the fovea by the finest ganglion cell array. But the plump cone inner segments ultimately occupy 40% of the photoreceptor sheet, and appear to impinge on the collecting area needed by rods (see Figs. 17.5 and 17.6). This problem seems solved when in dim light the pupil enlarges, allowing much of the light to enter peripheral cones at high angles to their optical

axes. Off-axis photons escape the light guide and spill into neighboring rods. Thus, although receptor ratios and dimensions are fixed, the proportion of light captured by cones and rods shifts adaptively with the optics of the eye. Peripheral cones *need* more light because the eye movements that steady an image on the foveal cones move the image across the peripheral cones, allowing less temporal integration (Eckert and Buchsbaum, 1993).

In summary, vertebrate photoreceptors exemplify the principle of symmorphosis: the mutual optimization of components across many levels. Here, we have considered the apportioning of: (1) space in the receptor mosaic; (2) outer segment volume; (3) numbers of key transduction proteins on a disc and their ratios; (4) reason for the disc; (5) number of cGMP-gated channels; (6) channel binding affinity, cooperativity, and partial blockage; and (7) inner segment size. These features all cooperate to set transduction efficiency, speed, gain, S:N, and bandwidth. They all match for a particular environmental state (e.g., starlight or daylight), and they compromise to promote overall performance (survival). These biophysical factors, by jointly setting the spatiotemporal integration of photons in a receptor, determine the size of its "information packet" to be relayed forward. This, in turn, determines many features of the downstream neural circuitry.

Transmitting the photoreceptor signal

ROD AXON IS THIN AND CONE AXON IS THICK Rod and cone axons are just long enough to traverse their nuclear layer and reach their synaptic targets. Typically, the distance is about 20 μm, but where their axons must course laterally to connect with second order neurons (near the fovea in primates), they are much longer, up to 500 μm (Polyak, 1941). Irrespective of length, the two axon types differ markedly in thickness. The rod axon is thin, about 0.45 μm in diameter, and invariant with species and retinal location; whereas the cone axon is thick, up to 1.6 μm, and varies across the retina, being thinner in the fovea and thicker toward the periphery (see Figs. 17.6 and 17.8). The 4-fold difference in diameter implies a 16-fold difference in cross-sectional area.

This sets the number of microtubules in the axon cross-section, because microtubules are evenly spaced at a specific density that is the same for both axons (see Fig. 17.8; Hsu et al., 1998). So, a cone axon has ~440 microtubules in its cross-section, whereas a rod axon has only ~35. The rod axon's smaller cross-sectional area also implies a 16-fold smaller volume. Volume of the rod axon terminal is also less than that of the cone axon terminal, so that the combined volume of the rod axon + terminal is less than the combined volume of the cone axon + terminal by 10-fold (Hsu et al., 1998). Were the rod signaling apparatus not appropriately diminished but equal to that of the cone, the vast number of rods (20 rods/cone) would double the retina's postreceptoral thickness. So there must be pressure to minimize "wire volume" and match it to information capacity (Hsu et al., 1998).

ROD TERMINAL CONTAINS ONE ACTIVE ZONE WHEREAS CONE TERMINAL CONTAINS MANY We expect axon diameter to correlate with some *electrical* feature, such as space constant, conduction velocity, and temporal bandwidth. However, models suggest that outside the fovea a thin axon could adequately serve the cone's known electrical properties (Hsu et al., 1998). Instead, axon diameter correlates with the number of active zones.[3] The thin rod axon supplies a small terminal with one active zone (Rao-Mirotznik et al., 1995); whereas the thick cone axon supplies a large terminal with many active zones (e.g., 17 in cat central retina, 20 in primate fovea, and 50 in primate periphery) (Fig. 17.9; Haverkamp et al., 2000). As the primate cone terminal enlarges from fovea to periphery, so does the axon (see Fig. 17.6). This rule (axon thickness proportional to number of active zones) also holds for bipolar axons in cat and mouse (see Fig. 17.13*C*; Cohen and Sterling, 1990; Tsukamoto et al., 2001).

Because photoreceptors are tonically depolarized, each active zone releases vesicles tonically, at rates that seem astonishingly high. For example, the cat rod terminal with one active zone is calculated to release ~80 vesicles/second (see Fig. 17.9*C*; Rao et al., 1994; Rao-Mirotznik et al., 1998; van Rossum and Smith, 1998), consistent with capacitance measurements of the salamander rod (Rieke and Schwartz, 1996). The cat cone terminal with 18 active zones (see Fig. 17.9*B*) is estimated to release ~1500 vesicles/second, consistent with noise measurements in turtle (Ashmore and Copenhagen, 1983). In these examples, transmitter release seems to match information capacity; that is, it is smaller in the rod terminal that transfers an irreducible binary signal (0 or 1 photon/integration time) and greater in the cone terminal that transfers a richer, graded signal (de Ruyter van Steveninck and Laughlin, 1996).

The cone's estimated 15-fold higher release rate apparently requires nearly 15-fold more microtubules. Because microtubules serve as "tracks" for molecular motors to shuttle supplies between cell body and synapse, it makes sense that a terminal whose vesicle release rate matches its information rate should also require a corresponding match of mechanisms for resupply. This observation implies another key constraint in retina, that *information capacity should match wire volume.*

---

[3] An active zone is the presynaptic site where synaptic vesicles dock near clusters of voltage-sensitive calcium channels.

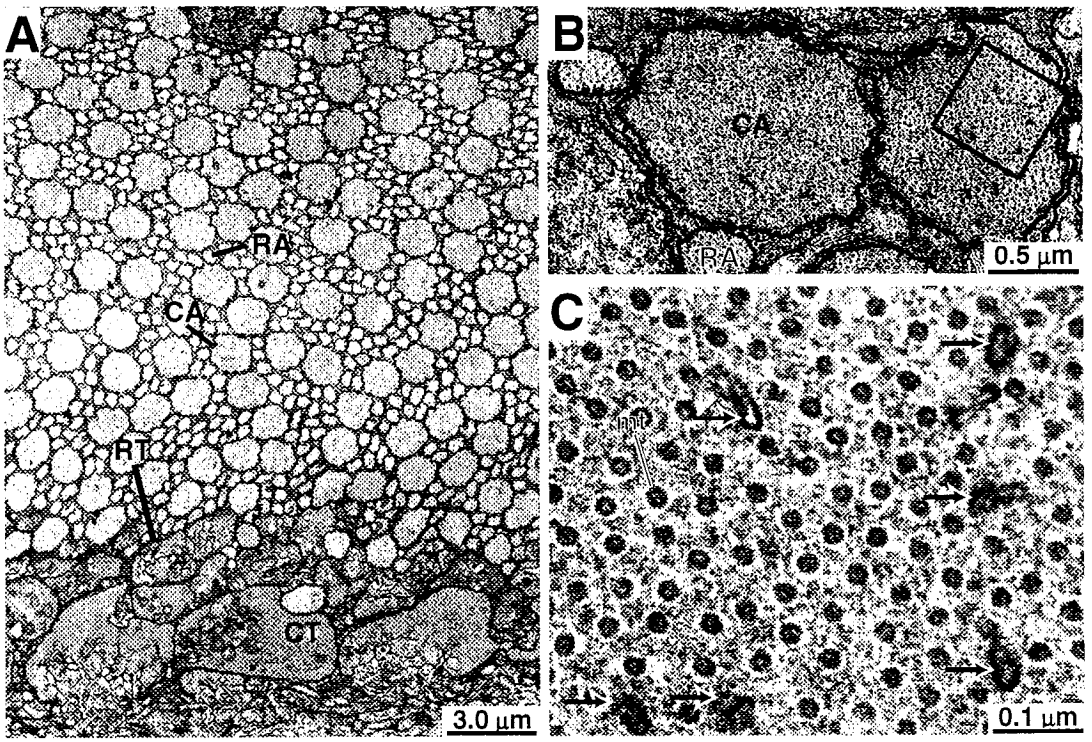

FIGURE 17.8. *A*, Electron micrograph of cross section through photoreceptor axons in macaque perifovea. Cone axons (CA) are 4-fold thicker than rod axons (RA). Cone terminals (CT) are also much larger than rod terminals (RT). *B*, Cone and rod axons are filled with microtubules at equal densities. The square indicates the region enlarged in *C*. *C*, Microtubules (mt) in the cone axon are evenly spaced and associated with patches of smooth membrane (*arrows*).

PHOTORECEPTOR SYNAPSES ARE STRUCTURALLY AND FUNCTIONALLY THREE-DIMENSIONAL A signal rich in information coupled to a channel of intrinsically limited capacity, would lose information (Laughlin, 1994). To prevent this, the photoreceptor synapse evolved several coding strategies: (1) compress the signal by bandpass filtering; (2) divide the filtered signal into multiple components and route them over parallel circuits with appropriately matched properties. For example, the weakest rod signals use a private, nonlinear circuit, whereas stronger rod and cone signals share a linear circuit. Strong signals sort further into circuits for different temporal bandwidth. To initiate these key steps in signal processing, the first synapse requires several types of lateral interneuron (horizontal cells) and also *many* types of relay neuron (bipolar cells). To connect with all these neurons while minimizing tissue volume, noise, and metabolic cost, photoreceptors employ a three-dimensional synapse (Haverkamp et al., 2000; Rao-Mirotznik et al., 1995; Vardi et al., 1998).

The synaptic ribbon tethers hundreds of vesicles and anchors to the plasma membrane. There, tens of vesicles along the base of the ribbon are apposed to the presynaptic membrane to form a linear active zone at the apex of an invagination that is 500 nm deep. The invagination houses multiple processes: two horizontal cell spines flank one or more bipolar dendrites (see Fig. 17.9). At the mouth of the invagination and tiling the base of the presynaptic terminal, other bipolar dendrites form specialized contacts: a few for the rod (Hack et al., 1999; Tsukamoto et al., 2001) and *hundreds* for the cone (see Fig. 17.9; Haverkamp et al., 2000).

When a vesicle containing ~10^3 glutamate molecules fuses at the apex of the invagination, some of the molecules diffuse rapidly across the 20-nm cleft to AMPA receptors on the horizontal cell spines. Other glutamate molecules diffuse more slowly down the 500-nm invagination to encounter mGluR6 glutamate receptors on the invaginating or "semi-invaginating" bipolar dendrites (see Fig. 17.9). Additional glutamate molecules diffuse still more slowly for 1000 nm or more to reach AMPA and kainate receptors on the "basal" bipolar dendrites that tile the terminal's base. Consequently, each vesicle delivers glutamate as a brief "pulse" or a slower "puff" to more than 10 (probably closer to 50) postsynaptic processes (DeVries, 2000; Haverkamp et al., 2000; Rao-Mirotznik et al., 1995, 1998).

This three-dimensional synaptic architecture confers two important advantages. First, by allowing every vesicle to affect many postsynaptic processes, the apparent cost of the photoreceptor's high basal rate of vesicle release is effectively reduced. Second, by allowing each active zone to affect

many postsynaptic processes, considerable synaptic divergence is achieved with minimum wire volume. Although many brain regions disallow "spillover" between synapses, the photoreceptors present a clear case where spillover is both extensive and deliberate; that is, it represents not a failure, but an intrinsic part of the design.

"Engineered spillover" requires that glial processes avoid the synaptic regions. For if the glia invaded, their transporters that rapidly bind and remove extracellular glutamate, would sharply restrict its spatiotemporal distribution (Lehre and Danbolt, 1998). Consequently, Müller glia avoid the invaginations and territory beneath the terminal (Burris et al., 2002; Sarantis and Mobbs, 1992). Glial membranes do wrap the photoreceptor axon and the upper surface of the terminal (see Fig. 17.9). They separate adjacent synaptic terminals except where the membranes are pierced by fine processes that form cone-cone and cone-rod gap junctions.

Three pathways divide the rod system's intensity range

In starlight the rod system employs many detectors but catches only a few photons, so the signal in each detector is binary: usually 0 and rarely 1. In moonlight the detectors still operate in binary mode, but with fewer 0s and more 1s. In twilight (or dawn) each detector catches more than one photon and thus has a coarsely graded signal. Each condition presents a different challenge for signal processing, each solved with a different circuit (Fig. 17.10).

STARLIGHT CIRCUIT: TWO STAGES OF CONVERGENCE EMPLOY NONLINEAR AMPLIFICATION The challenge in starlight is to separate the small signal in one rod from the continuous dark noise in many rods. The voltage evoked by one photon rises above the dark noise only modestly, by a factor of ~4 (Baylor

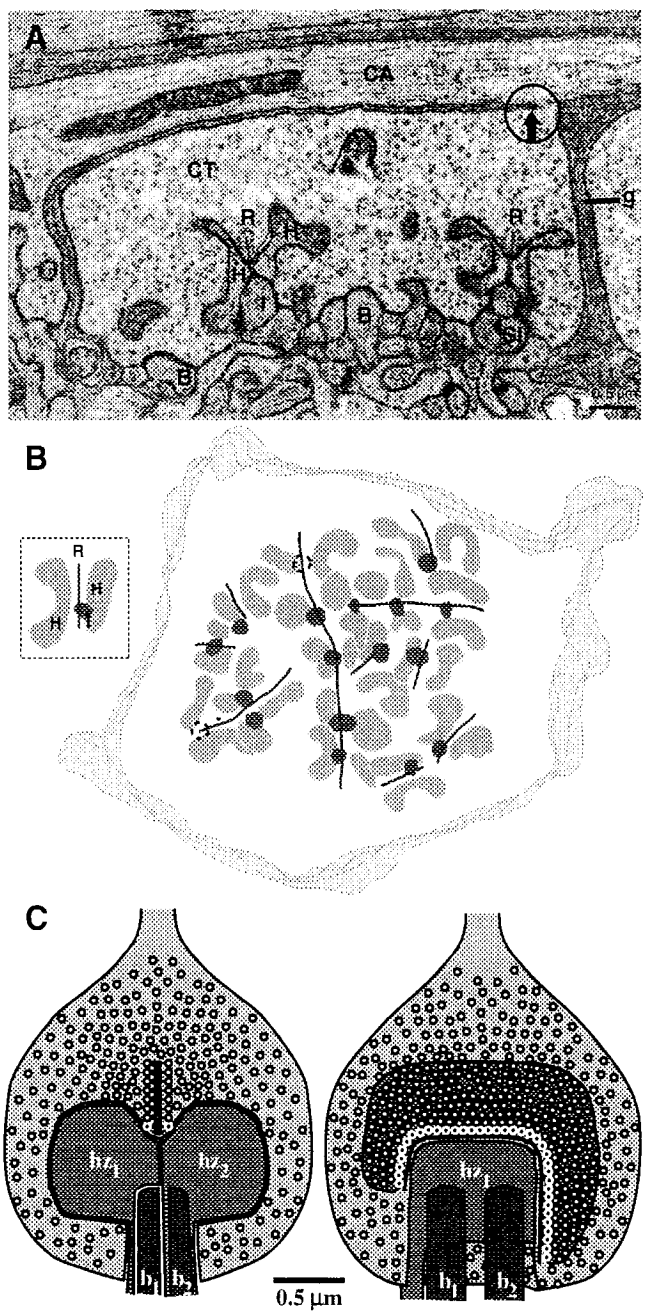

FIGURE 17.9. The cone uses many ribbon synapses to transmit a graded signal; the rod uses one ribbon to transmit a binary signal. *A,* Ultrathin section (~90 nm) through a macaque fovea cone terminal. Two ribbons (R) and their postsynaptic triads (H, H, I) are present, but full reconstruction shows 20 triads. At the base, semi-invaginating (SI) and basal (B) dendrites are also shown; full reconstruction shows several hundred such dendrites. The circled arrow indicates the gap junction with the adjacent terminal. Full reconstruction shows that every terminal connects to all its neighbors. Glial wrappings (g) separate the terminals, but avoid the terminal's secretory region, consistent with "engineered spillover" of each vesicle to many postsynaptic processes. *B,* Cone terminal in tangential view, reconstructed from electron micrographs of serial sections (cat central area). Inset shows a triad:ribbon (R) with an ON bipolar dendritic tip (dark spot) flanked by two horizontal cell spines (H). The terminals contain 11.6 ± 0.9 ribbons. These vary in length from 0.2 to 3.5 µm, but the total length per terminal is remarkably constant (9.9 ± 0.9 µm; N = 8). This provides a constant number of docking sites for synaptic vesicles (~600) and a still larger "depot" of vesicles tethered to the faces of the ribbon (~3000). The cone terminal has 17 triads. Short ribbons serve a single triad; long ribbons serve up to 5 triads. *C,* Rod terminal in orthogonal views (from three-dimensional reconstruction, cat central area). A single tetrad is present, with one ribbon pointing between two horizontal cell processes (hz) toward two rod bipolar dendrites (b). Note that the bipolar dendrites are hundreds of nanometers distant from docked vesicles. (*A,* Electron micrograph from Tsukamoto et al., 1992, with permission. *B,* From Harkins & Sterling, unpublished work. *C,* From Rao-Mirotznik et al., 1995, with permission.)

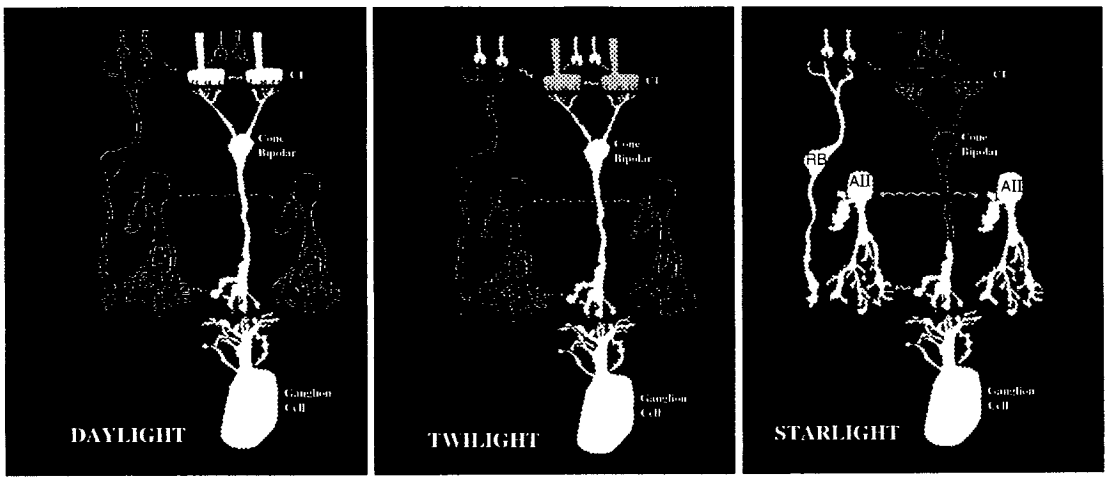

FIGURE 17.10. The final common pathway to the ganglion cell is served by three circuits. In daylight, cone signals are graded and thus require many ribbon synapses for transfer (both at the outer plexiform layer [OPL] and the inner plexiform layer [IPL]). In twilight, rod signals are graded and also require many ribbon synapses. Rods access these synapses by turning on their gap junctions to cone terminals, in effect "parasitizing" the multiple ribbon synapses available at both stages of the cone bipolar circuit. In starlight, rod signals are binary and thus require only one ribbon synapse (see Fig. 17.9*C*). The single photon response cannot transfer via coupling to the cone terminal because the many rods lacking a photon add too much noise. Therefore, the rod-cone junction may turn off to transfer the binary signal via the rod's ribbon synapse to the rod bipolar cell. The latter's response will be coarsely graded over some part of the intensity range (owing to rod convergence) and will thus require multiple ribbon synapses, which are present in the rod bipolar terminal. The AII cell's response will be more finely graded (owing to rod bipolar convergence), and will thus require yet more ribbon synapses. The AII cell gains access to these by turning on its gap junctions with cone bipolar terminals. Coupling of the AII cells—indirectly via the cone bipolar terminals and also directly via AII-AII junctions—spreads current widely enough to enlarge the ganglion cell's summation area well beyond its dendritic tree. This improves the S:N ratio in very dim light, but would degrade acuity in brighter light. Therefore, both sets of junction are regulated and presumably uncouple in twilight and daylight. See text for further explanation. (Modified from Sterling, 1998.)

et al., 1984). But the next neuron in the circuit, the rod bipolar cell, pools input from many rods ($\mathbf{n}$ = 20 to 120). If the rod synapse were linear, noise in the bipolar cell would rise as $\sqrt{\mathbf{n}}$ and swamp the single-photon event (Baylor et al., 1984). The problem could be solved by a nonlinear synapse that selectively amplified larger signals. This would effectively remove the dark noise by "thresholding," but at the cost of also removing single-photon events on the small end of the amplitude distribution (van Rossum and Smith, 1998). This mechanism has now been confirmed experimentally and shown to improve overall sensitivity compared to linear transfer (Fig. 17.11; Field and Rieke, 2002).

Of course, signals in each rod bipolar cell are also sparse and each has noise. So the circuit must converge tens of rod bipolar cells onto a second-stage interneuron, the AII amacrine cell, without swamping the signal (see Fig. 17.10). Again the solution involves a nonlinearity: larger rod bipolar inputs are selectively amplified by voltage-sensitive sodium channels in the AII cell (Boos et al., 1993; Smith and Vardi, 1995). Then AII cells send current via gap junctions to depolarize ON cone bipolar terminals. Simultaneously the AII also releases inhibitory transmitter (glycine) to hyperpolarize the OFF cone bipolar terminals and OFF ganglion cells. The overall circuit allows a single photon event to evoke a discrete "firing event" (1 to 3 spikes) in several ON ganglion cells and to suppress an equal number of spikes in several OFF ganglion cells (Barlow et al., 1971; Mastronarde 1983).

MOONLIGHT CIRCUIT: LINEAR CHEMICAL SYNAPSE ONTO OFF CONE BIPOLAR As photon density rises slightly, a second rod pathway comes into play. Some rods synapse on dendrites of an OFF cone bipolar cell (Hack et al., 1999; Soucy et al., 1998; Tsukamoto et al., 2001). This synapse amplifies linearly and thus transfers all photon events, which when summed, exceed the noise (see Fig. 17.11*C*; Field and Rieke, 2002; Sterling, 2002). Although only a few rods manage to contact a cone bipolar dendrite, the small gap junctions between rod terminals might couple them at this intensity to pool the signals (see Fig. 17.11; Tsukamoto et al., 2001). This pathway has been found so far only in rodents.

TWILIGHT CIRCUIT: ROD ELECTRICAL SYNAPSE ONTO CONE When photon density reaches one photon/rod/ integration time (twilight, dawn), rod signals are processed by cone circuits (see Fig. 17.10). Each rod terminal forms gap junctions with two cone terminals, and every cone terminal is

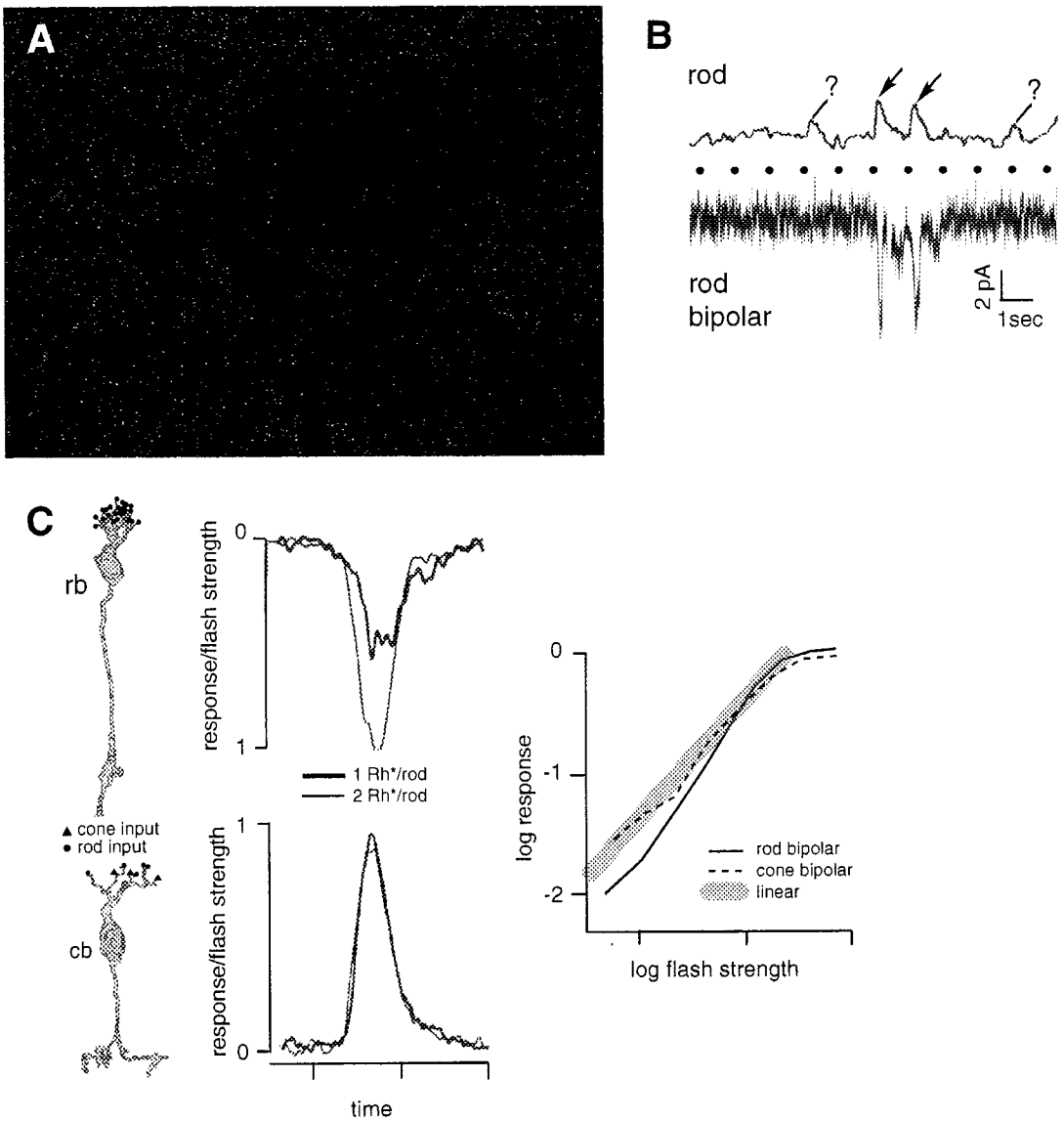

FIGURE 17.11. *A*, Faint image of a baboon in starlight painted by photons in "pointillist" fashion. The probability of each pixel receiving a photon is governed by Poisson distribution, the mean of which corresponds roughly to the intensities used by Field and Rieke (2002). *B*, Single photon event in a rod rises clearly above the continuous noise (*arrows*) only when it is considerably larger than average. The same event in the rod bipolar cell is faster, with a much improved signal-to-noise ratio. The dotted trace represents flash timing. *C*, *Left*, A rod bipolar (rb) cell collects chemical synapses from 20 rods, whereas the cone bipolar (cb) cell collects from only a few rods. However, each rod probably pools signals from neighboring rods via gap junctions. *Middle*, Response amplitudes normalized for flash intensity. The cone bipolar response doubles for twice the intensity, but the rod bipolar response more than doubles. *Right*, Input/output curve for the cone bipolar cell is essentially linear, in contrast to that for the rod bipolar cell, which is clearly nonlinear. (*A*, Image courtesy of A. Hsu and R. Smith. *C*, neurons, reprinted from Tsukamoto et al., 2001; responses replotted from Field and Rieke, 2002.)

contacted by ~40 rods (Smith et al., 1986; Sterling et al., 1988). The rod signal (recognized by its spectral peak and time course) is observed in recordings from the cone (Nelson, 1977; Schneeweis and Schnapf, 1995, 1999). Rod signals are also present in horizontal cells whose dendrites do not contact rods (Nelson, 1977). Thus, electrical coupling from many rods to each cone allows the graded rod signal to be filtered and relayed by the same circuits used by the graded cone signals. This design reduces wire volume and metabolic cost.

Daylight circuit requires "bandpass filter" at the cone synapse

Recall that most sensory systems convert a receptor cell's graded potential into action potentials, either directly or

after interpolating a single synapse (see Fig. 17.3). But this requires special mechanisms that precede or accompany transduction to filter out noise and redundant signals. For example, the auditory, vestibular, and somatosensory systems employ complex mechanical filters before transduction to select particular temporal frequencies. And the olfactory and taste senses use more than 1000 different heptahelical receptors to select particular chemical stimuli (Zhang and Firestein, 2002). The eye employs only mild optical filtering,[4] and cones employ relatively minor molecular filtering (2 to 3 heptahelical receptors) to divide spectral bandwidth. Lacking vigorous preneural filtering or extensive molecular filtering by the transducer, the retina requires neural circuits to perform spatial and temporal bandpass filtering at the first synapse (Fig. 17.12).

The photovoltage arriving at the cone synaptic terminal spreads to neighboring cone terminals. This coupling filters noise intrinsic to the cones. In "steady" light, the cone voltage fluctuates owing to photon noise and biochemical noise arising from the transduction cascade. These noise sources are independent between cones, whereas the signals are locally correlated between cones owing to correlations in the visual scene plus optical blur. Therefore coupling reduces noise more than the signal. For a coupling strength of about 1 nS, neural blur in human fovea is narrower than the optical blur. Yet, because it gives the cone a slightly broader receptive field than the cone's optical aperture, it is detectable psychophysically. This lowpass filtering is calculated to improve the S:N ratio by about 60% at the cone terminal for spatial frequencies below 20 cycles/degree (DeVries et al., 2002).

The other essential step is to attenuate signals that are broadly correlated across cones. Correlations arise from the coarse structure in an image (low spatial and temporal frequencies) which delivers similar intensities to neighboring cones. (Think of a blackboard or a uniformly bright wall, or any spatial pattern that is temporally invariant.) These broadly correlated signal components carry little information about image structure and are therefore redundant. Removing them allows the cone synapse to use its dynamic range for what is essential, the *differences* between adjacent regions. In the jargon of signal processing, such filtering is termed "background subtraction", "contrast enhancement", or "highpass filtering". The theory for optimally matching the spatiotemporal bandpass filter to ambient light intensity is well developed (Srinivasan et al., 1982; van Hateren, 1992).

This essential integrative step is accomplished by the horizontal cell, which collects synaptic input from many cones (see Fig. 17.12). The horizontal cell's spines invaginate the cone terminal, forming the paired, lateral elements of the triad where they express AMPA receptors (see Fig. 17.9*A*; Haverkamp et al., 2001). The horizontal cell pools its signal electrically with neighboring cells. These connections produce a broad receptive field that represents a slightly delayed, center-weighted average of the cone membrane potential. Many diurnal mammals (e.g., cat, rabbit, and guinea pig) express two types of horizontal cell that connect to the same cones. One type is narrow-field with weaker coupling, the other is broad-field with stronger coupling (reviewed by Mills and Massey, 1994; Vaney, 1993) The two patterns of connection cause correspondingly different weighting functions, but they both project negative feedback onto the cone terminal and bipolar dendrites, creating a receptive field surround with the proper overall weight (see Fig. 17.12; Smith, 1995).

The negative sign of this feedback arises from gamma-aminobutyric acid (GABA), which the horizontal cells synthesize and release via an unconventional mechanism (Schwartz, 1987). These cells lack synaptic vesicles but release the transmitter by reverse action of a GABA transporter, apparently the vesicular GABA transporter (VGAT), which at conventional synapses loads GABA into vesicles (Haverkamp et al., 2000). GABA acts at the bipolar cell dendritic tips which express $GABA_A$ and $GABA_C$ receptors (Haverkamp et al., 2000; Vardi et al., 1992). These ligand-gated chloride channels pose an important puzzle: although GABA's function is to antagonize the stimulus, light depolarizes some bipolar cells (ON cells) and hyperpolarizes others (OFF cells). So how can the same receptor molecule mediate opposite effects? The current idea is that ON bipolar dendrites express a cotransporter that *accumulates* chloride (NKCC), and OFF bipolar dendrites express a cotransporter that *extrudes* chloride (KCC2). This would set E_{Cl} for the two bipolar classes on opposite sides of the membrane potential, so that GABA would drive their voltages in opposite directions (Vardi et al., 2000). Experimental support for this idea is so far underwhelming (Satoh et al., 2001; Billups and Attwell, 2002).

The cone terminal itself may express a $GABA_A$ receptor, but this remains controversial (Pattnaik et al., 2000; Picaud et al., 1998). A different mechanism, perhaps equally controversial, has been proposed for horizontal cell feedback

[4] Optical blur attenuates spatial frequencies greater than can be resolved bhy the cone array. For example, optics in the human fovea cut off frequencies above 60 cycles/degree. This precisely matches the foveal sampling rate (120 cones/degree), given Nyquist's rule that there must be one detector for each half cycle. Although it might seem counterintuitive that optical blur could *improve* vision, frequencies higher than the sampling rate would be seen as lower frequencies, and thus cause a kind of noise termed "aliasing" (Williams, 2003). The matching of optics to cone sampling rate further exemplifies the principle of symmorphosis.

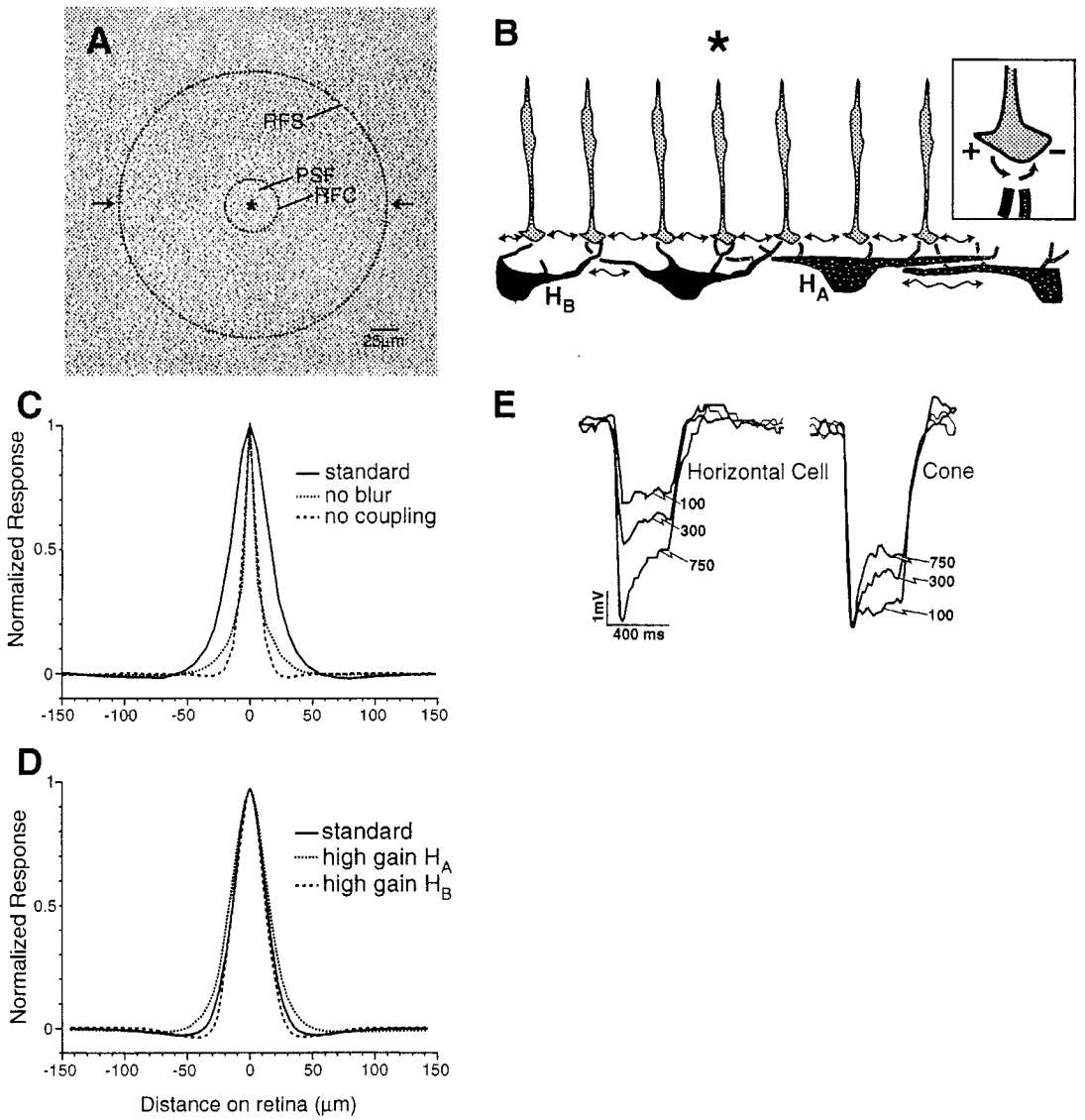

FIGURE 17.12. A center-surround receptive field ("bandpass filter") arises at the cone terminal. *A*, Cone array, cat central area (24,000/mm^2). A point of light striking the cornea spreads, owing to optical blur (PSF, point spread function), to stimulate about 10 cones. The signal spreads further, via coupling at cone terminals, creating a receptive field center (RFC) for one cone (*) that encompasses about 50 cones. Inhibitory feedback via horizontal cells creates a receptive field surround (RFS) encompassing about 1200 cones. *B*, Neural circuit that shapes the cone receptive field. The arrow between the terminals denotes coupling; the surround is shaped by inhibitory feedback (*inset*). *C*, Calculated sensitivity across the cone receptive field (area between arrows in *A*). To achieve the proper spatial weight requires both optical blur and cone-cone coupling. For surround; narrow, deep region set by the narrow-field H_B cell; broad, shallow region set by the wide-field H_A cell. *D*, Calculated sensitivity as presented in *C*. *E*, Intracellular recordings from squirrel retina. Enlarging a bright spot over a horizontal cell, from 100 μm to 750 μm in diameter, gives progressively larger responses. The same sequence, when applied to a cone, gives the greatest response to a small spot (100 μm) and rising attenuation (somewhat delayed) to larger spots. (*A to D*, Adapted from Smith, 1995. *E*, Adapted from Leeper and Charlton, 1985.)

onto the cone terminal (Kamermans et al., 2001). The horizontal cell spine expresses a gap junction channel protein (connexin), but does not form a gap junction with the opposing cone membrane. This dab of connexin is thought to be a hemichannel, observed previously in isolated horizontal cells (Devries and Schwartz, 1992). The idea is that when the horizontal cell depolarizes, releasing GABA onto bipolar dendrites, it also injects negative current into the extracellular space near the cone terminal's voltage-sensitive calcium channels. This reduces the calcium current and thus the cone terminal's synaptic gain (Kamermans et al., 2002). How these apparently disparate mechanisms cooperate to remove redundant information from the cone terminal remains to be determined.

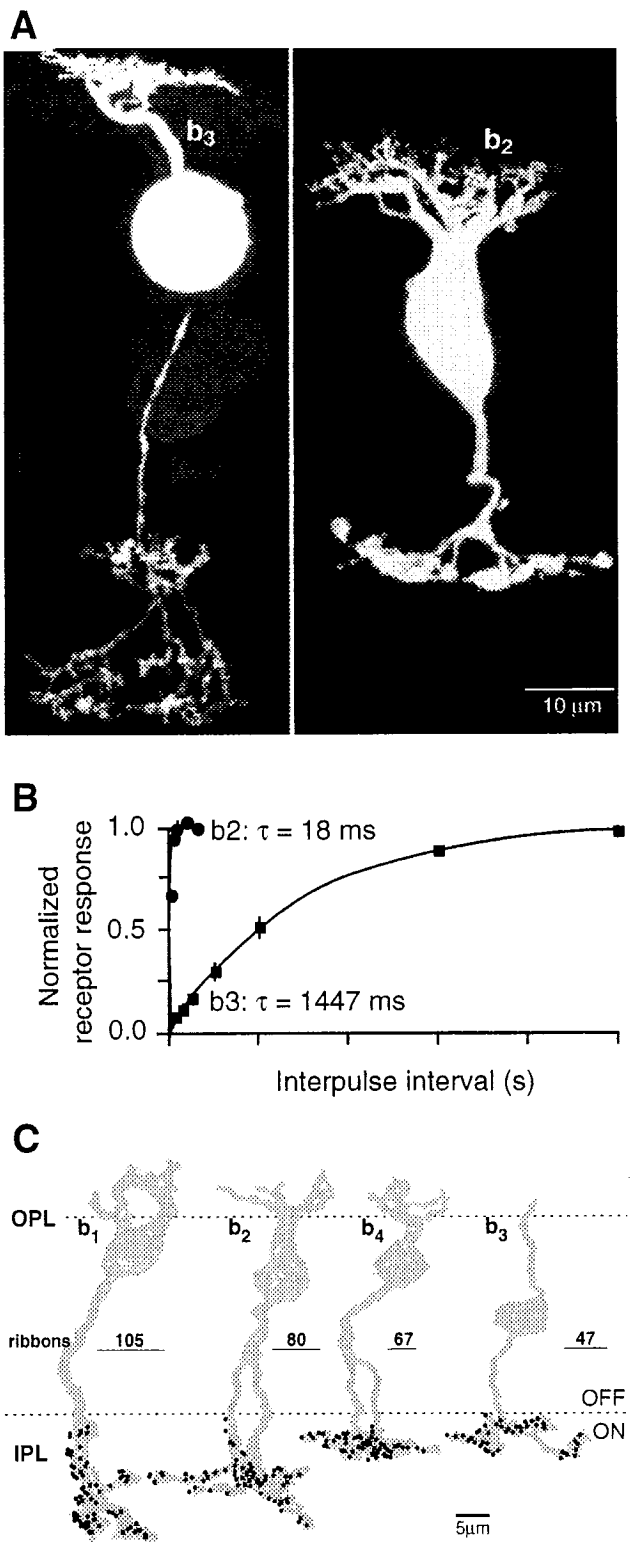

FIGURE 17.13. Two types of OFF cone bipolar cell (b3, b2) from a ground squirrel. *A*, Differences in axon caliber predict few ribbon outputs for b3 and more for b2. *B*, The difference also predicts higher temporal bandwidth for b2. Consistent with this, b2 shows much faster recovery from receptor desensitization, measured by removing the bipolar cells from a slice and measuring paired-pulse responses using a rapid perfusion system. *C*, ON cone bipolar cells (b1 to b4) from cat. Axons decrease in diameter from left to right, expressing fewer ribbons. OPL, outer plexiform layer; IPL, inner plexiform layer. (*A* and *B*, From S. DeVries, unpublished. *C*, Modified from Cohen and Sterling, 1990.)

Ten bipolar pathways (!) divide the cone signal

In daylight, the cone system uses relatively few detectors but catches many photons, so the signal in each detector (derived from 10^3 to 10^6 photons) is finely graded. This challenges neural circuitry in a manner opposite to the rod system, not with sparse information, but with a plethora. Even after bandpass filtering, the information in a cone signal exceeds the coding capacity of a single second-order neuron. The solution is to divide the signal into different components and transmit them to the inner retina over multiple circuits (Boycott and Wässle, 1991; Cohen and Sterling, 1990; Euler et al., 1996; Kolb et al., 1981; McGillem and Dacheux, 2001; McGuire et al., 1984).

The contrast signal created by horizontal cell filtering is halved at the cone output[5] (see Figs. 17.2, 17.4, and 17.12). Signals dimmer than the mean depolarize one class of bipolar cell (OFF cells), and signals brighter than the mean depolarize another class (ON cells). To achieve this, the cone releases glutamate simultaneously onto both bipolar classes, while their dendrites sense it with different receptors. The OFF bipolar dendrites express ionotropic receptors that *open* a cation channel; whereas the ON bipolar dendrites express a metabotropic receptor that *closes* a cation channel. The metabotropic receptor is mGluR6 (Masu et al., 1995; Nomura et al., 1994), which couples to $G_{\alpha o1}$ (Dhingra et al., 2000; 2002a), but the rest of the cascade and the channel itself remain elusive.

OFF signals are routed to 3 to 5 types of bipolar cell (Fig. 17.13). The purpose is to divide the signal into different temporal components. In one bipolar type the excitatory postsynaptic current (EPSC) is slow and sustained; in another type it is intermediate; and in a third type it is fast and transient. These kinetic differences arise because the cone's tonic release of glutamate strongly desensitizes iGluR receptors, and the particular iGluRs expressed on each cell type recover

[5] Such circuits must have evolved quite early as they are present even in sharls, the most primitive fish.

at different rates (Fig. 17.13*B*) (DeVries, 2000; DeVries and Schwartz, 1999). The OFF dendrites all contact the base of the cone terminal, but apparently at different distances from the sites of vesicle release: dendrites with large, fast currents are nearest, and dendrites with small, slow currents are farthest (DeVries, personal communication).

ON signals are also routed to five bipolar types, and for the same reason: to divide the signal into slow and fast components (see Fig. 13*B*; Cohen and Sterling, 1990; Freed, 2000a). However, since ON dendrites express only one isoform of mGluR6, the temporal differences must arise differently than in the OFF system. One idea is that the calcium influx through the ON bipolar cation channel, which antagonizes the response (Nawy, 2000), might have different kinetics in each cell type (Awatramani and Slaughter, 2000). This is known to be true for photoreceptors. Further kinetic shaping of the bipolar responses certainly occurs at their axon terminals, owing to autofeedback onto group III metabotropic glutamate receptors and to extrinsic feedback from amacrine processes that release GABA onto $GABA_C$ receptors (Awatramani and Slaughter, 2001; Euler and Masland, 2000; Freed et al., 2003).

Bipolar Axons End in Different Strata: Structure Matches Information Contet The two major classes of bipolar axon segregate at different levels of the inner plexiform layer, thus dividing it into OFF and ON laminae. Furthermore, within a lamina, each type of bipolar axon occupies a defined stratum, which can be quite thin (~2 μm) (see Fig. 17.13). This implies that the inner plexiform layer finely stratifies temporal information, which can be further sharpened by amacrine circuits that extend laterally in fine strata (Roska and Werblin, 2001). Some of these signals are transmitted rapidly and regeneratively over long distances (millimeters) by spiking amacrine cells (Cook et al., 1998; Demb et al., 1999; Stafford and Dacey, 1997).

Because a channel's information content rises directly with bandwidth (Shannon and Weaver, 1949), the bipolar types that signal higher temporal frequencies convey more information. The structural correlates are the same as for the rod and cone. Low frequency ("sustained") bipolar cells have thinner axons with fewer ribbon synapses (~50 to 80); whereas high frequency ("transient") bipolar cells have thicker axons with more synapses (~100 to 120) (Calkins et al., 1994; Cohen and Sterling, 1990; Tsukamoto et al., 2001). The slowest, poorest signal of all belongs to the rod bipolar cell, which has the thinnest axon and fewest ribbon synapses (20 to 40) (Ghosh et al., 2001; McGuire et al., 1984; Tsukamoto et al., 2001).

Design of ganglion cell circuits

Certain Ganglion Cells Select ON or OFF Inputs, but Other Types Combine Them

Bipolar axons at the inner plexiform layer deliver packets of information pooled from 5 to 10 cones. These graded signals are further pooled at the ganglion cell and re-encoded as spikes for transmission down the optic nerve. The specific pooling decisions are crucial because they irrevocably set the spatial and temporal resolution of all later stages. These decisions partly reflect the constraints already mentioned (dynamic range, noise, wire volume, and metabolic cost). But ganglion cells project to diverse brain regions that use different regions of the spatiotemporal frequency spectrum. Because further efficiencies can be achieved by matching the message to the "end user," ganglion cells are diverse, comprising some 10 to 20 types (Masland, 2001; O'Brien et al., 2002).

The separate ON and OFF channels established at the cone terminal are retained by ganglion cells. This is straightforward because bipolar cells employ ribbon synapses to release glutamate onto ganglion cell dendrites, and the latter always express iGluR receptors. Therefore, to collect either ON or OFF signals, a ganglion cell simply restricts its dendrites to either the upper or lower stratum of the inner plexiform layer. Indeed, many ganglion cell types continue to encode only the brighter or dimmer half of the contrast range. This is useful because the dynamic range of a neuron's spike-coding mechanism is limited, and this doubles the dynamic range available to encode contrast. Furthermore, to double the contrast range with one neuron, its spike number would need to rise 4-fold, a metabolically costly strategy (Attwell and Laughlin, 2001; von der Twer and MacLeod, 2001).

Certain ganglion cells break this rule by sending one set of dendrites to the OFF layer and another to the ON layer. For example, one ganglion cell collects synapses from an ON bipolar cell with exclusively S-cone input (sensitive to short wavelengths) and additional synapses from OFF bipolar cells with M- and L-cone input (sensitive to ***m***iddle and ***l***ong wavelengths). This wiring renders the cell most sensitive to light rich in short wavelengths and least sensitive to light rich in middle and long wavelengths (Calkins et al., 1998; Chichilnisky and Baylor, 1999; Dacey and Lee, 1994; Martin et al., 1997). By encoding a spectrally opponent signal (colloquially, "blue minus yellow"), this cell discards spectrally redundant information that in a "generalist" ganglion cell occupies considerable dynamic range and metabolic energy. The spectrally filtered signal is clearly optimized for its particular end user, the koniocellular layer of the lateral geniculate nucleus, which projects to "color circuits" in striate cortex (as reviewed in Calkins and Sterling, 1999).

"Brisk" Ganglion Cells Comprise Narrow-field and Wide-field Types More than half of all ganglion cells fire "briskly" (Fig. 17.14). The spike autocorrelograms rise steeply, and the peak rates are high, more than 100

spikes/second (Cleland and Levick, 1974a; DeVries and Baylor, 1997). The axons of brisk cells are relatively thick and rapidly conducting (e.g., Kirk et al., 1975; Rowe and Stone, 1976a), so their wire volume occupies more than 95% of the optic nerve's cross section (Sterling, unpublished).

About 90% of brisk cells have narrow dendritic fields that collect from relatively few bipolar cells. Transient and sustained bipolar types both contribute, and accordingly, the narrow-field ganglion cell responds to both stimulus components (Cohen and Sterling, 1992; Freed, 2000b). Narrow-field ganglion cells tile the retina (independently for both ON and OFF types), and because they sample space most densely and project 1 : 1 to parvocellular geniculate neurons, these two cell types set spatial acuity for their main end users, namely, simple cells in striate cortex (Smallman et al., 1996; Wässle and Boycott, 1991).

About 10% of the brisk cells have wide dendritic fields that collect from many bipolar cells. The wide-field ganglion cell is 3-fold broader than the narrow-field cell at the same retinal locus and thus collects from nearly 10-fold more bipolar cells—all of the transient type—and nearly 10-fold more bipolar synapses (Freed, 2000a ; Freed and Sterling, 1988; Kier et al., 1995). This design has several important consequences for the end users (superior colliculus and magnocellular pathways of the geniculostriate system). First, summing from many cones via many bipolar cells and bipolar synapses, the wide-field cell, compared to the narrow-field cell, has better S:N ratio and thus greater contrast sensitivity (Kaplan and Shapley, 1986). Threshold for the wide-field, brisk-transient ganglion cell to a spot over its dendritic field can be as low as 0.8% contrast (Dhingra et al., 2003). Second, wide spatial summation reduces sensitivity to high spatial frequencies (which are more effectively carried by narrow-field cells). This frees the cell's limited dynamic range to encode higher *temporal* frequencies and thus to match the input provided by transient bipolar cells (see Figs. 17.4 and 17.14).

A third consequence of wide-field summation is that the ganglion cell responds vigorously to a fine stimulus that reverses contrast or moves within the dendritic field (see Fig. 17.14; Hochstein and Shapley, 1976). Although the *array* of wide-field cells cannot detect fine detail when it is stationary (Fig. 17.4), the individual wide-field ganglion cell responds sensitively when the grating flickers or drifts (see Fig. 17.14). This serves end users, such as neurons in cortical area MT that detect motion based on changes in luminance and contrast (Demb et al., 2001a, 2001b). This response property is termed "nonlinear" because brightening one region while dimming another evokes a vigorous response, whereas in a linear system (such as the narrow-field ganglion cell) the two changes simply cancel.

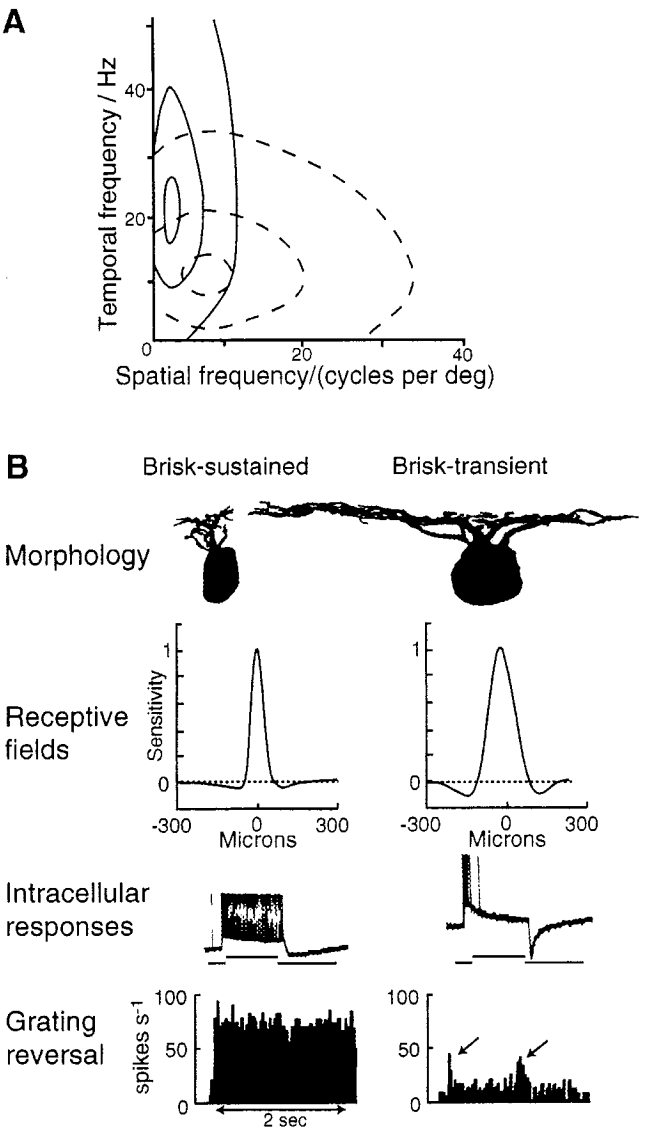

FIGURE 17.14. *A*, The spatiotemporal transfer function of the brisk-transient and brisk-sustained pathways. Contours are at 0.1, 0.5, and 0.9 of the maximum values. The brisk-sustained pathway is tuned to higher spatial frequencies and lower temporal frequencies. *B*, Radial views of ON brisk-sustained (narrow-field) and ON brisk-transient (wide-field) ganglion cells. The narrow-field cell collects 150 synapses (total) from several bipolar cells of each type (b1 to b4 in Fig. 17.12*C*). Because the bipolar cells have receptive fields broader than their spacing, their rectified responses cancel in the narrow-field ganglion cell and give no response to reversal of a fine grating. The wide-field cell collects about 600 synapses from about 150 bipolar cells, mostly from the transient bipolar cell (b1 in Fig. 17.12). Because the bipolar receptive fields are narrower than the large convergent array, the wide-field cells respond at each grating reversal (*arrows*). This "frequency doubling" arises because the rectified responses of individual bipolar cells are collected across such a wide field that they cannot cancel (Demb et al., 2001a). (*A*, Reprinted from Eckert and Buchsbaum, 1993. *B*, Modified from Sterling, 1998. Intracellular records from Saito, 1983. Spike histograms from Hochstein and Shapley, 1976.)

The nonlinear mechanism was initially attributed to amacrine circuits because bipolar circuits were thought to be linear. But we now know that the bipolar cell synapse expresses an important nonlinear property, "rectification". The bipolar synapse releases vesicles at a low basal rate; consequently, depolarization can increase release, but hyperpolarization cannot decrease it. Therefore, dimming an OFF bipolar cell increases release but brightening does not decrease it (and vice versa for an ON bipolar cell). This nonlinearity hardly affects a narrow-field ganglion cell because the bipolar receptive fields overlap due to cone coupling (Cohen and Sterling, 1992; Smith and Sterling, 1990). However, it strongly affects a wide-field cell because bipolar receptive fields are smaller than the extent of the convergent array (Demb et al., 2001a; Freed and Sterling, 1988). This important property of wide-field cells, which arises simply from their extent of spatial convergence, may be the clearest example at the circuit level of an "emergent property".

SLUGGISH GANGLION CELLS: SMALLER, SLOWER, CHEAPER Nearly half of the ganglion cells fire "sluggishly." Their spike autocorrelograms show a gradual rise and plateau, and their peak rates are ~10-fold lower than for brisk cells (Cleland and Levick, 1974a; DeVries and Baylor, 1997). The axons of sluggish cells are thin and slowly conducting (Stone and Fukuda, 1974). Consequently their wire volume is minimal, occupying less than 5% of the optic nerve's cross-section (Sterling, unpublished). Sluggish cells (also termed "W") comprise many types with complex response properties, such as directional selectivity and local-edge detection (e.g., Caldwell and Daw, 1978; Cleland and Levick, 1974b; Rowe and Stone, 1976a, 1976b).

Sluggish types have been relatively little studied, partly because when compared to types that fire briskly these cells seem somehow disadvantaged. Yet, this might actually imply a different coding strategy (Meister and Berry, 1999; Victor, 1999). A cell that responds only to motion of a local edge at low velocity carries fewer possible messages than a cell that responds to a wider range of stimuli. The simpler message might be encoded efficiently by fewer spikes that cost less in energy and in wire volume (Attwell and Laughlin, 2001; Ames and Li, 1992; Ames et al., 1992; Balasubramanian and Berry, 2002). For these benefits, slower conduction velocity seems to be an acceptable cost.

IS INFORMATION CONTENT THE SOLE DETERMINANT OF WIRE VOLUME? The hypothesis that wire volume matches information content arouses a healthy skepticism and thus needs some elaboration. The hypothesis tries to unify three facts: (1) axon thickness rises with number of output synapses; (2) the neurons with thicker axons and more outputs are the ones that transmit higher temporal frequencies; (3) higher temporal frequencies transmit more information. Points 1 and 2 are illustrated in FIGURES 17.8, 17.13, and 17.14; point 3 comes from Shannon's equation. The hypothesis claims that more synapses are required at the output because the information capacity of the synapse is limited (de Ruyter van Steveninck and Laughlin, 1996; Laughlin 1994).

Of course, there may be other reasons why a neuron might need additional synapses and thus a larger axon. For example, the brisk-transient ganglion cell (but not the brisk-sustained cell) typically sends one branch to innervate the lateral geniculate nucleus and another branch to the superior colliculus. Thus, its greater axon thickness may be partly attributable to its greater number of boutons in the geniculate and partly to its need to support an additional arbor. In short, the hypothesis does not exclude additional determinants of wire volume.

Conclusion

Many features of retinal design seem interpretable as evolutionary adaptations to a surprisingly small number of lifestyle decisions and physical constraints:

1. Because mammals move fast, their photoreceptors must be small. Because mammals forage night and day, they need both rods and cones. So rods must be numerous and information-poor, whereas cones can be sparse and information-rich.

2. The two receptor arrays require different circuits. Rods must converge in large numbers—yet not accumulate noise that would swamp their information-poor signals. This requires several stages, each equipped to remove noise by nonlinear amplification. Cones must converge in smaller numbers—yet not allow their information-rich signals to saturate postsynaptic neurons. This requires bandpass filtering to reduce redundancy and noise.

3. The retina must remain thin and cannot increase its metabolic rate. Therefore rod and cone circuits must jointly minimize total cellular volume and metabolic cost. Indeed, each circuit seems constrained to expend these quantities in proportion to its information content.

Some additional circuits (mainly amacrine) are known but not described here, and many additional amacrine circuits remain to be discovered. But quite likely their purposes will prove generally similar: to optimize signal transfer using various forms of neural adaptation or gain control. Many of the matches suggested here under the rubric of symmorphosis lack quantitative rigor. This suggests the next large task: to quantify, for each retinal circuit, its information rate, metabolic cost, and wire volume, and to test quantitatively the relationships between these three variables. When this is accomplished, the retina will finally be "understood."

Acknowledgments

I thank Drs. Robert Smith, Martin Wilson, and David Vaney for comments on the manuscript, and Sharron Fina for preparing it. My research has been supported by NEI grants EY00828 and EY08124. I thank Drs. Steven DeVries and Amy Harkins for providing unpublished data for Figures 17.9 and 17.13.

REFERENCES

Adam, G., and M. Delbrück, 1968. Reduction of dimensionality in biological diffusion processes, in Structural Chemistry and Molecular Biology, (A. Rich and N. Davidson eds.), San Francisco CA: W. H. Freeman & Company.

Ames, A. I., and Y. -Y. Li, 1992. Energy requirements of glutamatergic pathways in rabbit retina. J. Neurosci., 12:4234–4242.

Ames, A. I., Y. -Y. Li, E. C. Heher, and C. R. Kimble, 1992. Energy metabolism of rabbit retina as related to function: high cost of Na^+ transport. J. Neurosci., 12:840–853.

Ashmore, J. F., and D. Copenhagen, 1983. An analysis of transmission from cones to hyperpolarizing bipolar cells in the retina of the turtle. J. Physiol., 340:569–597.

Attwell, D., 1986. The Sharpey-Schafer Lecture: ion channels and signal processing in the outer retina. Q. J. Exp. Physiol. 71:497–536.

Attwell, D., and S. Laughlin, 2001. An energy budget for signaling in the grey matter of the brain. J. Cerebr. Blood F. Met., 21:1133–1145.

Awatramani, G. B., and M. M. Slaughter, 2000. Origin of transient and sustained responses in ganglion cells of the retina. J. Neurosci., 20:7087–7095.

Awatramani, G. B., and M. M. Slaughter, 2001. Intensity-dependent, rapid activation of presynaptic metabotropic glutamate receptors at a central synapse. J. Neurosci., 21:741–749.

Baseler, H. A., A. A. Brewer, L. T. sharpe, A. B. Moreland, H. Jagle, and B. A. Wandell, 2002. Reorganization of human cortical maps caused by inherited photoreceptor abnormalities. Nat. Neurosci., 5:364–370.

Balasubramanian, V., and M. J. Berry II, 2002. A test of metabolically efficient coding in the retina. Network 13:531–552.

Barlow, H. B., W. R. Levick, and M. Yoon, 1971. Responses to single quanta of light in retinal ganglion cells of the cat. Vision Res., S3:87–101.

Baylor, D. A., T. D. Lamb, and K.-W. Yau, 1979. Responses of retinal rods to single photons. J. Physiol., 288:613–634.

Baylor, D. A., B. J. Nunn, and J. L. Schnapf, 1984. The photocurrent, noise and spectral sensitivity of rods of the monkey Macaca fascicularis. J. Physiol., 357:575–607.

Billups, D., and D. Attwell, 2002. Control of intracellular chloride concentration and GABA response polarity in rat retinal ON bipolar cells. J. Physiol. 545:183–198.

Boos, R., H. Schneider, and H. Wässle, 1993. Voltage- and transmitter-gated currents of AII-amacrine cells in a slice preparation of the rat retina. J. Neurosci., 13:2874–2888.

Boycott, B. B., and H. Wässle, 1991. Morphological classification of bipolar cells of the primate retina. Eur. J. Neurosci., 3:1069–1088.

Burns, M. E., and D. A. Baylor, 2001. Activation, deactivation, and adaptation in vertebrate photoreceptor cells. Annu. Rev. Neurosci., 24:779–805.

Burns, M. E., and T. D. Lamb, 2003. Visual transduction by rod and cone photoreceptors, in Visual Neurosciences, (L. Chalupa and J. S. Werner eds.), Cambridge MA:MIT Press.

Burris, C., K. Klug, I.-T. Ngo, P. Sterling, and S. Schein, 2002. How Müller glial cells in macaque fovea coat and isolate the synaptic terminals of cone photoreceptors. J. Comp. Neurol. 453:100–111.

Caldwell, J. H., and N. W. Daw, 1978. New properties of rabbit retinal ganglion cells. J. Physiol., 276:257–276.

Calkins, D. J., S. Schein, Y. Tsukamoto, and P. Sterling, 1994. M and L cones in Macaque fovea connect to midget ganglion cells via different numbers of excitatory synapses. Nature, 371:70–72.

Calkins, D. J., and P. Sterling, 1999. Evidence that circuits for spatial and color vision segregate at the first retinal synapse. Neuron, 24:313–321.

Calkins, D. J., Y. Tsukamoto, and P. Sterling, 1998. Microcircuitry and mosaic of a blue/yellow ganglion cell in the primate retina. J. Neurosci., 18:3373–3385.

Calvert, P. D., V. I. Govardovskii, N. Krasnoperova, R. E. Anderson, J. Lem, and C. L. Makino, 2001. Membrane protein diffusion sets the speed of rod phototransduction. Nature, 411:90–94.

Chichilnisky, E. J., and D. A. Baylor, 1999. Receptive-field microstructure of blue-yellow ganglion cells in primate retina. Nat. Neurosci., 2:889–893.

Cleland, B. G., and W. R. Levick, 1974a. Brisk and sluggish concentrically organized ganglion cells in the cat's retina. J. Physiol. (Lond.), 240:421–456.

Cleland, B. G., and W. R. Levick, 1974b. Properties of rarely encountered types of ganglion cells in the cat's retina and an overall classification. J. Physiol., 240:457–492.

Cohen, E., and P. Sterling, 1990. Demonstration of cell types among cone bipolar neurons of cat retina. Philos. Trans. R. Soc. Lond. B, 330:305–321.

Cohen, E., and P. Sterling, 1992. Parallel circuits from cones to the on-beta ganglion cell. Eur. J. Neurosci., 4:506–520.

Cook, P. B., P. D. Lukasiewicz, and J. S. McReynolds, 1998. Action potentials are required for the lateral transmission of glycinergic transient inhibition in the amphibian retina. J. Neurosci., 18:2301–2308.

Curcio, C. A., K. R. Sloan, R. E. Kalina, and A. E. Hendrickson, 1990. Human photoreceptor topography. J. Comp. Neurol., 292:497–523.

Curcio, C. A., K. R. Jr. Sloan, O. Packer, A. E. Hendrickson, and R. E. Kalina, 1987. Distribution of cones in human and monkey retina: Individual variability and radial asymmetry. Science, 236:579–582.

Dacey, D. M., and B. B. Lee, 1994. The "blue-on" opponent pathway in primate retina originates from a distinct bistratified ganglion cell type. Nature, 367:731–735.

de Ruyter van Steveninck, R., and S. B. Laughlin, 1996. The rate of information transfer at graded-potential synapses. Nature, 379:642–645.

Demb, J. B., K. Zaghloul, L. Haarsma, and P. Sterling, 2001a. Bipolar cells contribute to nonlinear spatial summation in the brisk transient (Y) ganglion cell in mammalian retina. J. Neurosci., 21:7447–7454.

Demb, J. B., L. Haarsma, M. A. Freed, and P. Sterling, 1999. Functional circuitry of the retinal ganglion cell's nonlinear receptive field. J. Neurosci., 19:9756–9767.

Demb, J. B., K. Zaghloul, and P. Sterling, 2001b. Cellular basis for the response to second-order motion cues in Y retinal ganglion cells. Neuron, 32:711–721.

DeVries, S. H., and E. A. Schwartz, 1992. Hemi-gap-junction channels in solitary horizontal cells of the catfish retina. J. Physiol. 445:201–230.

DeVries, S. H., 2000. Bipolar cells use kainate and AMPA receptors to filter visual information into separate channels. Neuron, 28:847–856.

DeVries, S. H., and D. A. Baylor, 1997. Mosaic arrangement of ganglion cell receptive fields in rabbit retina. J. Neurophysiol., 78:2048–2060.

DeVries, S. H., X. Qi, R. G. Smith, W. Makous, and P. Sterling, 2002. Electrical coupling between mammalian cones. Curr. Biol. 12:1900–1907.

DeVries, S. H., and E. A. Schwartz, 1999. Kainate receptors mediate synaptic transmission between cones and "Off" bipolar cells in a mammalian retina. Nature, 397:157–160.

Dhingra, A., M. Jiang, T.-L. Wang, A. Lyubarsky, A. Savchenko, T. Bar-Yehuda, P. Sterling, L. Birnbaumer, and N. Vardi, 2002. Light response of retinal ON bipolar cells requires a specific splice variant of Gαo. J. Neurosci., 22:4878–4884.

Dhingra, A., A. Lyubarsky, M. Jiang, E. N. Jr. Pugh, L. Birnbaumer, P. Sterling, and N. Vardi, 2000. The light response of ON bipolar neurons requires $G_{\alpha o}$. J. Neurosci., 20:9053–9058.

Dhingra, N. K., Y.-H. Kao, P. Sterling, and R. G. Smith, 2003. Contrast threshold of a brisk-transient ganglion cell. (Submitted).

Diamond, J., 1993. Evolutionary physiology, in The Logic of Life, (C. A. R. Boyd and D. Noble eds.), New York:Oxford University Press: pp. 89–111.

Diamond, J., and K. Hammond, 1992. The matches, achieved by natural selection, between biological capacities and their natural loads. Experientia, 48:551–557.

Diamond, J. M., 1992. The red flag of optimality. Nature, 355:204–206.

Eckert, M. P., and G. Buchsbaum, 1993. Efficient coding of natural time varying images in the early visual system. Philos. Trans. R. Soc. Lond. B, 339:385–395.

Enoch, J. M., 1981. Retinal receptor orientation and photoreceptor optics. Vertebrate photoreceptor optics. (J. M. Enoch and F. L. Tobey Jr. eds), Berlin: Springer-Verlag.

Euler, T., and R. H. Masland, 2000. Light-evoked responses of bipolar cells in a mammalian retina. J. Neurophysiol., 83:1817–1829.

Euler, T., H. Schneider, and H. Wässle, 1996. Glutamate responses of bipolar cells in a slice preparation of the rat retina. J. Neurosci., 16:2934–2944.

Field, G. D., and F. Rieke, 2002. Nonlinear signal transfer from mouse rods to bipolar cells and implications for visual sensitivity. Neuron, 34:773–785.

Freed, M. A., 2000a. Parallel cone bipolar pathways to ganglion cell use different rates and amplitudes of quantal excitation. J. Neurosci., 20:3956–3963.

Freed, M. A., 2000b. Rate of quantal excitation to a retinal ganglion cell evoked by sensory input. J. Neurophysiol., 83:2956–2966.

Freed, M. A., R. G. Smith, and P. Sterling, 2003. Timing of quantal release from the retinal bipolar terminal is regulated by a feedback circuit. (Submitted).

Freed, M. A., and P. Sterling, 1988. The ON-alpha ganglion cell of the cat retina and its presynaptic cell types. J. Neurosci., 8:2303–2320.

Ghosh, K. K., S. Haverkamp, and H. Wässle, 2001. Glutamate receptors in the rod pathway of the mammalian retina. J. Neurosci., 21:8636–8647.

Glegg, G. L., 1969. The Design of Design, Cambridge: University of Cambridge.

Gould, S. J., and R. C. Lewontin, 1979. The spandrels of San Marcos and the Panglossian paradigm: a critique of the adaptationist program. Proc. R. Soc. Lond. B 205:581–598.

Greeff, R., 1899. Die Mikroskopische Anatomie Des Sehnerven Und Der Netzhaut, Leipzig: W. Engelmann.

Hack, I., L. Peichl, and J. H. Brandstätter, 1999. An alternative pathway for rod signals in the rodent retina: Rod photoreceptors, cone bipolar cells, and the localization of glutamate receptors. Proc. Natl. Acad. Sci. USA, 96:14130–14135.

Haverkamp, S., U. Grünert, and H. Wässle, 2000. The cone pedicle, a complex synapse in the retina. Neuron, 27:85–95.

Haverkamp, S., U. Grünert, and H. Wässle, 2001. The synaptic architecture of AMPA receptors at the cone pedicle of the primate retina. J. Neurosci., 21:2488–2500.

Hochstein, S., and R. M. Shapley, 1976. Linear and nonlinear spatial subunits in Y cat retinal ganglion cells. J. Physiol. (Lond.), 262:265–284.

Hsu, A., Y. Tsukamoto, R. G. Smith, and P. Sterling, 1998. Functional architecture of primate rod and cone axons. Vision Res., 38:2539–2549.

Hughes, A., 1977. The topography of vision in mammals of contrasting life style: comparative optics and retinal organisation, in Handbook of Sensory Physiology, (F. Crescitelli ed.), Berlin: Springer-Verlag: pp. 615–756.

Kamermans, M., I. Fahrenfort, K. Schultz, U. Janssen-Bienhold, T. Sjoerdsma, and R. Weiler, 2001. Hemichannel-mediated inhibition in the outer retina. Science, 292:1178–1180.

Kamermans, M., I. Fahrenfort, and T. Sjoerdsma, 2002. GABAergic modulation of ephaptic feedback in the outer retina. IOVS, Abstract #2920.

Kaplan, E., and R. M. Shapley, 1986. The primate retina contains two types of ganglion cells, with high and low contrast sensitivity. Proc. Natl. Acad. Sci. USA 83:2755–2757.

Kier, C. K., G. Buchsbaum, and P. Sterling, 1995. How retinal microcircuits scale for ganglion cells of different size. J. Neurosci., 15:7673–7683.

Kirk, D. L., B. G. Cleland, and W. R. Levick, 1975. Axonal conduction latencies of cat retinal ganglion cells. J. Neurophysiol., 38:1395–1402.

Kolb, H., R. Nelson, and A. Mariani, 1981. Amacrine cells, bipolar cells and ganglion cells of the cat retina: a Golgi study. Vision Res., 21:1081–1114.

Koshland, D. E. Jr., A. Goldbeter, and J. B. Stock, 1982. Amplification and adaptation in regulatory and sensory systems. Science, 217:220–225.

Kraft, T. W., D. M. Schneeweis, and J. L. Schnapf, 1993. Visual transduction in human rod photoreceptors. J. Physiol., 464:747–765.

Lamb, T. D., and E. N. Jr. Pugh, 1992. G-protein cascades: Gain and kinetics. Trends Neurosci., 15:291–298.

Laughlin, S. B., 1994. Matching coding, circuits, cells, and molecules to signals: General principles of retinal design in the fly's eye. Prog. Ret. & Eye Res., 13:165–196.

Leeper, H. F., and J. S. Charlton, 1985. Response properties of horizontal cells and photoreceptor cells in the retina of the tree squirrel, Sciurus carolinensis. J. Neurophysiol., 54:1157–1166.

Lehre, K. P., and N. C. Danbolt. 1998. The number of glutamate transporter subtype molecules at glutamatergic synapses: chem-

ical and stereological quantification in young adult rat brain. J. Neurosci., 18:8751–8757.

Lamb, T. D., E. N. Pugh Jr., and V. Y. Arshavsky, 2000. The gain of rod phototransduction: reconciliation of biochemical and electrophysiological measurements. Neuron 27:525–537.

Leskov, I. B., V. A. Klenchin, J. W. Handy, G. G. Whitlock, V. I. Govardovskii, M. D. Bownds, T. D. Lamb, E. N. Pugh, V. Y. Arshavsky, 2000. The gain of rod phototransduction: reconciliation of biochemical and electrophysiological mearurements. Neuron, 27:525–537.

Liebman, P. A., K. R. Parker, and E. A. Dratz, 1987. The molecular mechanism of visual excitation and its relation to the structure and composition of the rod outer segment. Annu. Rev. Physiol., 49:765–791.

Martin, P. R., A. J. White, A. K. Goodchild, H. D. Wilder, and A. E. Sefton, 1997. Evidence that blue-on cells are part of the third geniculocortical pathway in primates. Eur. J. Neurosci., 9:1536–1541.

Masland, R. H., 2001. The fundamental plan of the retina. Nat. Neurosci., 4:877–886.

Mastronarde, D. N., 1983. Correlated firing of cat retinal ganglion cells. I. Spontaneously active inputs to X- and Y-cells. J. Neurophysiol., 49:303–324.

Masu, M., H. Iwakabe, Y. Tagawa, T. Miyoshi, M. Yamashita, Y. Fukuda, H. Sasaki, K. Hiroi, Y. Nakamura, and R. Shigemoto, 1995. Specific deficit on the ON response in visual transmission by targeted disruption of the mGluR6 gene. Cell, 80:757–765.

McGillem, G. S., and R. F. Dacheux, 2001. Rabbit cone bipolar cells: Correlation of their morphologies with whole-cell recordings. Vis. Neurosci., 18:675–685.

McGuire, B. A., J. K. Stevens, and P. Sterling, 1984. Microcircuitry of bipolar cells in cat retina. J. Neurosci., 4:2920–2938.

Meister, M., and M. J. I. Berry, 1999. The neural code of the retina. Neuron, 22:435–450.

Miller, W. H., and A. W. Snyder, 1973. Optical function of human peripheral cones. Vision Res., 13:2185–2194.

Mills, S. L., and S. C. Massey, 1994. Distribution and coverage of A- and B-type horizontal cells stained with Neurobiotin in the rabbit retina. Vis. Neurosci., 11:549–560.

Nakatani, K., T. Tamura, and K. -W. Yau, 1991. Light adaptation in retinal rods of the rabbit and two other nonprimate mammals. J. Gen. Physiol., 97:413–435.

Nawy, S., 2000. Regulation of the On bipolar cell mGluR6 pathway by Ca^{2+}. J. Neurosci., 20:4471–4479.

Nelson, R, 1977. Cat cones have rod input: a comparison of the response properties of cones and horizontal cell bodies in the retina of the cat. J. Comp. Neurol., 172:109–136.

Nomura, A., R. Shigemoto, Y. Nakamura, N. Okamoto, N. Mizuno, and S. Nakanishi, 1994. Developmentally-regulated postsynaptic localization of a metabotropic glutamate-receptor in rat rod bipolar cells. Cell, 77:361–369.

O'Brien, B. J., T. Isayama, R. Richardson, and D. M. Berson, 2002. Intrinsic physiological properties of cat retinal ganglion cells. J. Physiol. 538:787–802.

Packer, O., A. Hendrickson, and C. Curcio, 1989. Photoreceptor topography of the retina in the adult pigtail Macaque (Macaca nemestrina). J. Comp. Neurol., 288:165–183.

Pattnaik, B., A. Jellali, J. Sahel, H. Dreyfus, and S. Picaud, 2000. $GABA_C$ receptors are localized with microtubule-associated protein 1B in mammalian cone photoreceptors. J. Neurosci., 20:6789–6796.

Petroski, H., 1996. Invention by Design: How Engineers Get From Thought to Thing, Cambridge MA: Harvard University Press.

Picaud, S., B. Pattnaik, D. Hicks, V. Forster, V. Fontaine, J. Sahel, and H. Dreyfus, 1998. $GABA_A$ and $GABA_C$ receptors in adult porcine cones: evidence from a photoreceptor-glia co-culture model. J. Physiol., 513:33–42.

Polyak, S. L., 1941. The Retina, University of Chicago Press.

Potts, A. M., D. Hodges, C. B. Shelman, K. J. Fritz, N. S. Levy, and Y. Mangnall, 1972. Morphology of the primate optic nerve. I. Method and total fiber count. Invest. Ophthalmol. Vis. Sci., 11:980–988.

Pugh, E. N. Jr., and T. D. Lamb, 1993. Amplification and kinetics of the activation steps in phototransduction. Biochim. Biophys. Acta, 1141:111–149.

Rao-Mirotznik, R., G. Buchsbaum, and P. Sterling, 1998. Transmitter concentration at a three-dimensional synapse. J. Neurophysiol., 80:3163–3172.

Rao-Mirotznik, R., A. Harkins, G. Buchsbaum, and P. Sterling, 1995. Mammalian rod terminal: Architecture of a binary synapse. Neuron, 14:561–569.

Rao, R., G. Buchsbaum, and P. Sterling, 1994. Rate of quantal transmitter release at the mammalian rod synapse. Biophys. J., 67:57–63.

Rieke, F., and E. A. Schwartz, 1996. Asynchromous transmitter release: control of exocytosis and endocytosis at the salamander rod synapse. J. Physiol., 493:1–8.

Rodieck, R. W., 1973. The Vertebrate Retina: Principles of Structure and Function, San Francisco CA: W. H. Freeman & Co.

Rose, A., 1973. Vision: Human and Electronic, New York NY: Plenum Press.

Roska, B., and F. Werblin, 2001. Vertical interactions across ten parallel, stacked representations in the mammalian retina. Nature, 410:583–587.

Rowe, M. H., and J. Stone, 1976. Conduction velocity groupings among axons of cat retinal ganglion cells, and their relationship to retinal topography. Exp. Brain Res., 25:339–357.

Rowe, M. H., and J. Stone, 1976. Properties of ganglion cells in the visual streak of the cat's retina. J. Comp. Neurol., 169: 99–126.

Saito, H.-A., 1983. Morphology of physiologically identified X-, Y-, and W-type retinal ganglion cells of the cat. J. Comp. Neurol. 221:279–288.

Sarantis, M., and P. Mobbs, 1992. The spatial relationship between Müller cell processes and the photoreceptor output synapse. Brain Res. 584:299–304.

Satoh, H., M. Kaneda, and A. Kaneko, 2001. Intracellular chloride concentration is higher in rod bipolar cells than in cone bipolar cells of the mouse retina. Neurosci. Lett. 310:161–164.

Schnapf, J. L., B. J. Nunn, M. Meister, and D. A. Baylor, 1990. Visual transduction in cones of the monkey Macaca fascicularis. J. Physiol., 427:681–713.

Schneeweis, D. M., and J. L. Schnapf, 1995. Photovoltage of rods and cones in the macaque retina. Science, 268:1053–1056.

Schneeweis, D. M., and J. L. Schnapf, 1999. The photovoltage of Macaque cone photoreceptors: adaptation, noise, and kinetics. J. Neurosci., 19:1203–1216.

Schwartz, E., 1987. Depolarization without calcium can release gamma-aminobutyric acid from a retinal neuron. Science, 238: 350–355.

Sesti, F., M. Straforini, T. D. Lamb, and V. Torre, 1994. Gating, selectivity and blockage of single channels activated by cyclic GMP in retinal rods of the tiger salamander. J. Physiol., 474: 203–222.

Shannon, C. E., and W. Weaver, 1949. The Mathematical Theory of Communication, Urbana: University of Illinois Press.

Smallman, H. S., D. I. A. MacLeod, S. He, and R. W. Kentridge, 1996. Fine grain of the neural representation of human spatial vision. J. Neurosci., 16:1852–1859.

Smith, R. G., 1995. Simulation of an anatomically-defined local circuit: The cone-horizontal cell network in cat retina. Vis. Neurosci., 12:545–561.

Smith, R. G., M. A. Freed, and P. Sterling, 1986. Microcircuitry of the dark-adapted cat retina: functional architecture of the rod-cone network. J. Neurosci., 6:3505–3517.

Smith, R. G., and P. Sterling, 1990. Cone receptive field in cat retina computed from microcircuitry. Vis. Neurosci., 5:453–461.

Smith, R. G., and N. Vardi, 1995. Simulation of the AII amacrine cell of mammalian retina: Functional consequences of electrical coupling and regenerative membrane properties. Vis. Neurosci., 12:851–860.

Snyder, A. W., S. B. Laughlin, and D. G. Stavenga, 1977. Information capacity of eyes. Vision Res., 17:1163–1175.

Soucy, E., S. Nirenberg, J. Nathans, and M. Meister, 1998. A novel signaling pathway from rod photoreceptors to ganglion cells in mammalian retina. Neuron, 21:481–493.

Srinivasan, M. V., S. B. Laughlin, and A. Dubs, 1982. Predictive coding: A fresh view of inhibition in the retina. Proc. R. Soc. Lond. B, 216:427–459.

Stafford, D. K., and D. Dacey, 1997. Physiology of the A1 amacrine: a spiking, axon-bearing interneuron of the macaque monkey retina. Vis. Neurosci., 14:507–522.

Steinberg, R. H., M. Reid, and P. L. Lacy, 1973. The distribution of rods and cones in the retina of the cat (Felis domesticus). J. Comp. Neurol., 148:229–248.

Sterling, P., 1998. Retina, in The Synaptic Organization of the Brain, (G. M. Shepherd ed.), New York:Oxford University Press: pp. 205–253.

Sterling, P., 2002. Needle from a haystack: optimal signaling by a nonlinear synapse. Neuron, 34:670–672.

Sterling, P., E. Cohen, R. G. Smith, and Y. Tsukamoto, 1992. Retinal circuits for daylight: why ballplayers don't wear shades, in Analysis and Modeling of Neural Systems, (F. H. Eeckman ed.), Kluwer Academic Publishers: Boston, pp. 143–162.

Sterling, P., M. A. Freed, and R. G. Smith, 1988. Architecture of the rod and cone circuits to the On-beta ganglion cell. J. Neurosci., 8:623–642.

Stone, J., and Y. Fukuda, 1974. Properties of cat retinal ganglion cells: a comparison of W-cells with X- and Y-cells. J. Neurophysiol., 37:722–748.

Tamura, T., K. Nakatani, and K.-W. Yau, 1991. Calcium feedback and sensitivity regulation in primate rods. J. Gen. Physiol., 98: 91–130.

Taylor, C. R., and E. R. Weibel, 1981. Design of the mammalian respiratory system. I. Problem and strategy. Respir. Physiol., 44:1–10.

Townes-Anderson, E., 1995. Intersegmental fusion in vertebrate rod photoreceptors. Rod cells structure revisisted. Invest. Ophthalmol. Vis. Sci. 36:1918–1933.

Townes-Anderson, E., P. R. MacLeish, and E. Raviola, 1985. Rod cells dissociated from mature salamander retina: ultrastructure and uptake of horseradish peroxidase. J. Cell Biol. 100:175–188.

Tsukamoto, Y., P. Masarachia, S. J. Schein, and P. Sterling, 1992. Gap junctions between the pedicles of macaque foveal cones. Vision Res. 32:1809–1815.

Tsukamoto, Y., K. Morigiwa, M. Ueda, and P. Sterling, 2001. Microcircuits for night vision in mouse retina. J. Neurosci., 21:8616–8623.

Van Essen, D. C., C. H. Anderson, and D. J. Felleman, 1992. Information processing in the primate visual system: An integrated systems perspective. Science, 255:419–423.

van Hateren, J. H., 1992. Real and optimal neural images in early vision. Nature 360:68–70.

van Hateren, J. H., 1993. Spatiotemporal contrast sensitivity of early vision. Vision Res., 33:257–267.

van Rossum, M. C. W., and R. G. Smith, 1998. Noise removal at the rod synapse of mammalian retina. Vis. Neurosci., 15:809–821.

Vaney, D. I., 1993. Patterns of neuronal coupling in the retina. Prog. Ret. & Eye Res., 13:301–355.

Vardi, N., P. Masarachia, and P. Sterling, 1992. Immunoreactivity to $GABA_A$ receptor in the outer plexiform layer of the cat retina. J. Comp. Neurol., 320:394–397.

Vardi, N., K. Morigiwa, T.-L. Wang, Y.-J. Shi, and P. Sterling, 1998. Neurochemistry of the mammalian cone 'synaptic complex'. Vision Res., 38:1359–1369.

Vardi, N., L.-L. Zhang, J. A. Payne, and P. Sterling, 2000. Evidence that different cation chloride cotransporters in retinal neurons allow opposite responses to GABA. J. Neurosci., 20:7657–7663.

Victor, J. D., 1999. Temporal aspects of neural coding in the retina and lateral geniculate. Network, 10:R1–R66.

von der Twer, T., and D. I. A. MacLeod, 2001. Optimal nonlinear codes for the perception of natural colors. Network, 12:395–407.

Watson, A. B., H. B. Barlow, and J. G. Robson, 1983. What does the eye see best? Nature, 302:419–422.

Wässle, H., and B. B. Boycott, 1991. Functional architecture of the mammalian retina. Physiol. Rev., 71:447–480.

Williams, D. R., 2003. Image formation and sampling, in Visual Neurosciences, (L. Chalupa and J. S. Werner eds.), Cambridge MA: MIT Press.

Williams, R. W., C. Cavada, and F. Reinoso-Suárez, 1993. Rapid evolution of the visual system: A cellular assay of the retina and dorsal lateral geniculate nucleus of the Spanish wildcat and the domestic cat. J. Neurosci., 13:208–228.

Yau, K.-W., 1994. Phototransduction mechanism in retinal rods and cones. Invest. Ophthalmol. Vis. Sci., 35:9–32.

Zhang, D. J., and S. Firestein, 2002. The olfactory receptor gene superfamily of the mouse. Nat. Neurosci., 5:124–133.